Secretome protein signature of human pancreatic cancer stem-like cells

Jessica Brandi [1], Elisa Dalla Pozza [2], Ilaria Dando [2], Giulia Biondani [2], Elisa Robotti [3], Rosalind Jenkins [4], Victoria Elliott [5], Kevin Park [4], Emilio Marengo [3], Eithne Costello [5], Aldo Scarpa [6], Marta Palmieri [2]*, Daniela Cecconi [1]

[1] University of Verona, Department of Biotechnology, Proteomics and Mass Spectrometry Laboratory, Verona, 37134, Italy;

[2] University of Verona, Department of Life and Reproduction Sciences, Verona, 37134, Italy;

[3] University of Piemonte Orientale, Department of Sciences and Technological Innovation, Alessandria, 15121, Italy;

[4] University of Liverpool, MRC Centre for Drug Safety Science, Department of Molecular & Clinical Pharmacology, Liverpool, L69 3GE, United Kingdom;

[5] NIHR Liverpool Pancreas Biomedical Research Unit, Department of Molecular and Therapeutic Cancer Medicine, Liverpool, L69 3GA, United Kingdom;

[6] University and Hospital Trust of Verona, Applied Research on Cancer Network (ARC-NET) and Department of Pathology and Diagnostics, Verona, 37134, Italy.

* Corresponding author: Professor Marta Palmieri, Department of Life and Reproduction Sciences, Section of Biochemistry, University of Verona, Strada Le Grazie 8, I-37134 Verona, Italy

Phone: +39 045 8027169; FAX: +39 045 8027170; e-mail: marta.palmieri@univr.it

ABSTRACT

Emerging research has demonstrated that pancreatic ductal adenocarcinoma (PDAC) contains a sub-population of cancer stem cells (CSCs) characterized by self-renewal, anchorage-independent-growth, long-term proliferation and chemoresistance. The secretome analysis of pancreatic CSCs has not yet been performed, although it may provide insight into tumour/microenvironment interactions and intracellular processes, as well as to identify potential biomarkers.

To characterize the secreted proteins of pancreatic CSCs, we performed an iTRAQ-based proteomic analysis to compare the secretomes of Panc-1 cancer stem-like cells (Panc1 CSCs) and parental cell line. A total of 72 proteins were found up-/down-regulated in the conditioned medium of Panc-1 CSCs. The pathway analysis revealed modulation of vital physiological pathways including glycolysis, gluconeogenesis and pentose phosphate pathway.

Through ELISA immunoassays we analysed the presence of the three proteins most highly secreted by Panc-1 CSCs (ceruloplasmin, galectin-3, and MARCKS) in sera of PDAC patient. ROC curve analysis suggests ceruloplasmin as promising marker for patients negative for CA19-9.

Overall, our study provides a systemic secretome analysis of pancreatic CSCs revealing a number of secreted proteins which participate in pathological conditions including cancer differentiation, invasion and metastasis. They may serve as a valuable pool of proteins from which biomarkers and therapeutic targets can be identified.

Introduction

Pancreatic ductal adenocarcinoma (PDAC) is one of the most aggressive and devastating human malignancies with a death-to-incidence ratio of 0.99. Most patients have metastatic disease at the time of diagnosis. More than 75% of patients who undergo surgical resection of small pancreatic tumours with clear surgical margins and no evidence of metastasis nonetheless die from metastasis within 5 years [1], a finding that is consistent with early spread. In addition to late diagnosis, high resistance to chemotherapy and radiation seems to be responsible for the dismal outcome of PDAC. Recent studies have demonstrated that in a mouse model of PDAC cellular dissemination leading to metastasis occurs prior to the formation of an identifiable primary tumour [2]. This behaviour is associated with epithelial-to-mesenchymal transition (EMT) and with the establishment of circulating pancreatic cells which maintain a mesenchymal phenotype and express typical markers of cancer stem cells (CSCs) [3]. Evidence for the existence of CSCs has also been provided in primary human pancreatic adenocarcinomas grown in immunocompromised mice [4]. At the present, PDAC CSCs may be considered a subpopulation of cells in the bulk of the tumour characterised by the exclusive ability to drive tumourigenesis and metastasis and to play a fundamental role in disease relapse. Hence, to substantially impact long-term survival of PDAC patients, the study of the biological features and of the secretome of PDAC CSCs is critical, and will inform the development of more efficient therapies and the identification of early biomarkers.

The high heterogeneity of CSCs, which originates from genotypic and phenotypic plasticity, and their low presence in cancer sample tissues make their isolation and correct identification extremely difficult, strongly limiting the realization of biochemical studies. The current approach to isolate CSCs from tissue samples is mainly based on the difference in cell size or on the expression of specific antigens. However, these methods do not permit the recovery of sufficient cells to perform proteome or

secretome studies. In order to obtain valid and reproducible results, the biochemical approach to CSC pathophysiology can take advantage of the observation that CSCs can be isolated and enriched from several human cancer cell lines [5]. Recently, our group has been able to isolate cancer stem-like cells from five out of nine PDAC cell lines [6]. In particular, we have demonstrated that Panc-1 cancer stem-like cells (Panc1 CSCs) isolated from parental cell line by using the CSC selective medium, represent a model of great importance to deepen the understanding of the biology of pancreatic adenocarcinoma. Panc-1 CSCs showed the highest tumorsphere-forming ability, were more resistant to the action of the anticancer drugs, had typical surface stem cell markers, and when subcutaneously injected into nude female mice were more tumorigenic than parental cells. Thus far, proteomic approaches have been applied to pancreatic CSCs isolated from xenografted tumours in mice [7], early stage tumours [8], or established cell lines [9]. However, secretome analysis of pancreatic CSCs has not yet been reported, although the secreted proteins may serve as a valuable tool to obtain insight into interaction of the tumour with its microenvironment as well as intracellular processes, taking into account the observation that many tumour cells shed intracellular and even nuclear proteins into the extracellular space. Furthermore, these studies may allow the identification of potential PDAC biomarkers. Contrarily to PDAC, secretome approaches have been used to investigate CSCs of colon [10] and prostate cancer [11]. In general, secretome studies on cell lines grown in culture medium are limited by contamination from intracellular proteins originating from spontaneous cell autolysis. For this reason, a filtering criterion [12] must be established to select bona fide secreted proteins while avoiding the contaminants for downstream validation works. In this study, we have adopted a shotgun proteomics approach using iTRAQ 8-plex coupled with 2D-LC-MS/MS to compare the secretome of Panc1 pancreatic adenocarcinoma cell line with that of their derived stem-like cells (Panc1 CSCs). In order to identify only secreted proteins, we have compared the protein expression levels of the conditioned medium (CM)

with those of the whole cell lysate, taking into account that the relative abundance of secreted proteins should be higher in CM than in cell lysate. Following this approach, we have identified 43 proteins secreted at higher level by Panc1 CSCs relative to the parental cells. *In silico* functional pathway analysis has demonstrated a predominant association of these proteins to glycolysis, gluconeogenesis, IGF-1 signalling, atherosclerosis signalling, pyruvate fermentation to lactate, and pentose phosphate pathway. Among the identified proteins, ceruloplasmin was the most abundant detected in CM from Panc1 CSCs and showed promise as predictors for PDAC, particularly for patients negative for CA19-9.

To our knowledge, this is the first proteomic study of pancreatic CSC secretome. Our findings advance the understanding of the pathways implicated in tumourigenesis, metastasis and chemoresistance of pancreatic cancer, and also identify a pool of proteins from which novel candidate diagnostic and therapeutic biomarkers could be discovered.

MATERIALS AND METHODS

Cell culture

The human PDAC cell line Panc1 was grown in RPMI 1640 supplemented with 10% FBS, 2 mM glutamine, and 50 µg/ml gentamicin sulfate (Gibco, Life Technologies). Adherent cells were maintained in standard conditions for a few passages at 37°C with 5% CO_2. Panc1 CSCs were obtained as previously described [6]. Briefly, adherent cells were cultured in CSC medium (i.e. DMEM/F-12 supplemented with glucose, B27, fungizone, penicillin/streptomycin, heparin, epidermal growth factor and fibroblast growth factor) for at least 1-3 weeks or until the appearance of tumorspheres, which were then cultured in CSC medium for at least three passages before initiating the experiments.

Sample preparation

Panc1 cells and Panc1 CSCs were grown to ~70% confluence in 150 cm^2 culture flasks, washed six times in serum-free RPMI and B27-free DMEM/F-12 medium, respectively, and then incubated in serum/B27-free medium for 22 h. Cell viability, determined with 0.4% trypan blue solution (Invitrogen), was higher than 95%. The media containing secreted proteins were collected by centrifugation at 1,000 x g for 10 min to pellet floating cells and were defined as conditioned media (CM). After the addition of 1x protease inhibitor cocktail, CM were centrifuged again at 100,000 x g for 20 min at 4°C to pellet the remaining cell debris. Proteins in the CM were precipitated overnight at -20°C with 4 volumes of ice-cold acetone. The pellets were then collected by centrifugation at 17,000 x g for 20 min at 4°C, resuspended in 0.5 M TEAB containing 0.1% SDS, and finally concentrated using 3kDa cut-off spin columns (Millipore). To obtain whole lysate samples, the cell pellets were collected and lysed in 0.5 M TEAB containing 0.1% SDS and 1x protease inhibitor cocktail. Cells were lysed by two steps of sonication (3 times for 10 sec) interposed with a step at -80°C for 30 min. Samples were then centrifuged at 14,000 x g for 10 min at 4°C to remove debris, and the supernatants were collected and stored at -80°C. Protein concentrations were determined using BCA protein assay (Thermo Scientific).

iTRAQ 8-plex labeling

The iTRAQ 8-plex reagents were purchased from AB Sciex (Framingham, USA) and the labeling was carried out following the protocol provided by the manufacturer. A set of Panc1 whole cell lysate and CM samples and Panc1 CSC whole cell lysate and CM samples was labeled with iTRAQ reagent 113, 114, 115, and 116, respectively. A second biological replicate from a different cell culture passage was prepared and labeled in the same order with iTRAQ reagents 117, 118, 119, and 121. Briefly, samples were prepared to have 100 µg of proteins in a final volume of 25 µl. Two µl of 0.05 M tris-(2-carboxyethyl) phosphine (TCEP) Reducing Agent (Sigma) were added to each sample and the

mixture was incubated at 60°C for 1 h. Then, 1 µl of Cysteine Blocking Reagent (Iodoacetamide, 15 mg/ml, Sigma) was added and the mixture was incubated at room temperature for 10 min. Finally, 10 µg of trypsin (Promega, Sequence Grade) were added to each tube and the samples were incubated at 37°C overnight for protein digestion. iTRAQ reagents were allowed to reach room temperature and 50 µl of isopropanol were added to each tube. Subsequently, the content of each iTRAQ reagent vial was transferred to each sample tube, and incubated for 2 h at room temperature. Finally, the labeled proteins were mixed and subjected to SCX chromatography to remove impurities and excess labels. The iTRAQ samples were diluted to 5 ml with diluent (10 mM potassium phosphate (KH_2PO_4), 25% acetonitirile), adjusted to pH 3 with H_3PO_4, and loaded onto a SCX chromatography column (4.6 x 200 mm, polysulfoethil A, PolyLC; Agilent 1200). Peptides were fractionated over a 90 min gradient at flow rate of 1 ml/min. Fractions (80 x 1ml) were collected at room temperature, vacuum dried and stored at 4°C. For de-salting processing of eluted fractions, each dried fraction was dissolved in 1 ml of 100% H_2O:0.1%TFA and loaded onto a RP C18 column (Agilent 4.60 mm x 50 mm) using a Vision HPLC (Perseptive Biosystems, UK). Peptides were washed for 10 min with 0.1 % TFA and then rapidly eluted using 100% ACN:0.1%TFA at flow rate of 1.5 ml/min using in-line column switching. Each desalted fraction was dried overnight by vacuum centrifugation and stored at 4°C.

LC-MS/MS analysis and data processing

Desalted fractions were reconstituted in 40 µL 0.1% formic acid and 5 µL aliquots were delivered into a Triple TOF 5600 (AB Sciex) via an Eksigent NanoUltra cHiPLC System (AB Sciex) mounted with a microfluidic trap (200 µm x 500 µm ChromXP C18-CL 3 µm 300 Å) and analytical column (15 cm × 75 µm) packed with ChromXP C_{18}−CL 3 µm. A NanoSpray III source was fitted with a 10 µm inner diameter SilicaTip emitter (New Objective, Woburn, USA). The trap column was washed

with 2% ACN/0.1% formic acid for 10 min at 2 μL/min. A gradient of 2−50% ACN/0.1% formic acid (v/v) over 90 min was applied at a flow rate of 300 nL/min. Spectra were acquired automatically in positive ion mode using information-dependent acquisition powered by Analyst TF 1.5.1 software (AB Sciex). Up to 25 MS/MS spectra were acquired per cycle (approximately 10 Hz) using a threshold of 100 counts per s and with dynamic exclusion for 12 s. The rolling collision energy was increased automatically by selecting the iTRAQ check box in Analyst, and manually by increasing the collision energy intercepts by 5. TOF-MS spectra were acquired for 250 ms (mass range 400−1650 Da) and MS/MS spectra for100 ms each (mass range 100−1400 Da). Mass spectrometer recalibration was performed at the start of every fifth sample using a β-galactosidase digest standard.

Data analysis was performed using ProteinPilot software (Version 4.2, revision 1340, AB Sciex) using default settings and with bias and background correction applied. The data were searched against UniProt/SwissProt database (2013_2, total 30,309,316 entries, 40,464 human entries searched) using the Paragon algorithm (4.2.0.0, version 1304, AB Sciex). The mass tolerance for both precursor and fragment ions was 10ppm. ProteinPilot uses an algorithm for its peptide identifications wherein there is not an option to select the number of missed or non-specific cleavages *per se*. Instead, it searches the databases using probabilities of cleavages at different residues depending on the enzyme used (trypsin: after Arg probability of 0.9, after Lys 0.8, after Lys-Lys 0.7 etc.) [13]. It also performs initial database matching based on short sequence tags, rather than on parent ion m/z, which means it is acceptable to include peptides with missed or non-specific cleavages if they are identified with sufficient confidence. These will then contribute to the overall confidence of protein identification. The variable modifications selected for the search were ‘biological modifications’ (probability-based modification search of 461 biological, chemical and artefactual modifications), while the fixed modifications were carbamidomethylation of cysteines, and iTRAQ modification of C-terminal lysine residues and peptide

N-termini. A global FDR value of 1% was used based on the number of proteins identified before 1% of the identifications were derived from a match to the reverse database [14] (equating to an unused score of 1.09 and a confidence of 91.9%). Similarly, a global FDR cut-off of 1% was used as the criterion for acceptance of individual MS/MS spectra and in this case corresponded to a confidence of 93.8%. Protein redundancy is also handled seamlessly in ProteinPilot via the ProGroup algorithm [13]. The software reports all peptides that contribute to protein identification, but the protein will only be listed in the results table if there are peptides unique to that protein within the dataset. Only unique peptides contribute to the quantification. The exception is when there is a family of proteins with multiple highly homologous isoforms. In some of these cases, a unique peptide cannot be detected in the dataset. Under these circumstances, the software selects a 'winner' based on which protein identification best explains the peptides observed. The quantification will be based on the peptides which are most discriminatory.

Ratios were calculated from the areas under the curve for each iTRAQ reporter ion selecting different denominators depending on the comparisons to be made. Mean ratios were calculated based on all occurrences (up to 7) of all peptides for which there was a peptide confidence of >15% and where the protein was confidently identified through other evidence. Where a single peptide was used for quantification, the peptide confidence cut-off was 95%. Where a single peptide was used for identification, the cut-off was 99%. The Paragon algorithm performs a Student t-test on the unweighted log ratios (for background corrected data) and reports the p-value: for a final error rate of 5% and with 1157 proteins quantified, the Bonferroni correction suggests a significant p-value at 0.0043.

Bioinformatics analysis of secretion pathways

The potential secretion pathways of proteins were predicted with the SecretomeP 2.0 server [15] (http://www.cbs.dtu.dk/services/SecretomeP/) for classical and nonclassical secretion. Protein sequences

were retrieved from the Uniprot database and uploaded onto the SecretomeP 2.0 server for prediction of protein secretion. Potential exosomal and microvesicle release of the proteins was studied by manual annotation on the ExoCarta exosome [16] (http://exocarta.ludwig.edu.au/) and Vesiclepedia [17] (http://microvesicles.org/index.html) databases.

Ingenuity Pathway Analysis

A bioinformatics approach was used to clarify the global implication of differentially secreted proteins in Panc1 cells and in Panc1 CSCs. The Ingenuity computational Pathway Analysis (IPA) (Ingenuity Systems, Redwood City, CA) software was applied to organize data into biological functions that are over represented, create molecular networks, and identify potentially perturbed molecular pathways. The IPA program uses a knowledge base derived from the literature to relate the proteins to each other based on their interaction and function. The knowledge base consists of a high-quality expert-curated database containing 1.5 million biological findings, including more than 42,000 mammalian genes and pathway interactions extracted from the literature. In brief, Ingenuity uses the Core Analysis module to rank the proteins into top biological functions, networks, as well as canonical pathways involved. The IPA analysis settings were as follows: i) Reference set: Ingenuity Knowledge Base; ii) Relationship to include: Direct and Indirect; iii) Filter Summary: Consider only molecules and/or relationships where (species = Human) AND (confidence = Experimentally Observed). Proteins associated with canonical pathways were estimated as significant using Fisher's exact test (p value < 0.01) to determine the probability that the association between identified proteins and a canonical pathway could be explained by chance alone.

Western Blot

Protein samples from two different biological replicates were diluted 1:1 with Laemmli's sample buffer (62.5 mM Tris-HCl, pH 6.8, 25% glycerol, 2% SDS, 0.01% Bromophenol Blue), boiled for 3 min and separated by SDS/polyacrylamide gel electrophoresis (PAGE) on 12% T acrylamide gels in Tris/glycine/SDS buffer. Proteins were then electroblotted onto polyvinilydene fluoride membranes (Bio-Rad, Hercules, CA) at 60 V for 2 h at 4°C. Ponceau S staining was used to confirm equal protein loading in different lanes. Non-specific sites were blocked by incubating the membranes with 5% non-fat dried milk and 0.05% Tween-20 (Sigma-Adrich) in Tris-buffered saline at 37°C for 45 min. Membranes were incubated with the different primary antibodies at the appropriate dilutions in 1% non-fat dried milk, 0.05% Tween-20 in Tris-buffered saline for 3 h at room temperature. Blots were then incubated 45 min at room temperature with the appropriate horseradish peroxidase (HRP)-conjugated secondary antibody (see the **Supplemental Table 1**). The immunocomplexes were visualized by chemiluminescence using the Chemidoc MP imaging system (Bio-Rad Laboratories) and the intensity of the chemiluminescence response was measured by processing the image with Quantity One software Version 4.5 (Bio-Rad).

Serum Samples

The protocols used for this study were approved by the Verona University Hospital Ethics Committee with informed patient consent. Serum samples from PDAC patients (n = 100, 1-4 TNM stages) were obtained from the archives of the Pancreas Institute, ARC-NET biobank of the Verona University Hospital G.B. Rossi (www.arc-net.it). Clinicopathological characteristics of the considered PDAC patients are shown in **Supplemental Table 2.** The healthy serum samples were obtained with informed consent from volunteers (n = 20) who received medical examinations at Verona University

Hospital G.B. Rossi. The number of cases and controls were chosen according to studies previously described by others [18, 19].

All of the samples were collected following a standardized protocol. The serum samples were prepared by collecting blood in empty tubes, which were maintained at room temperature for a minimum of 30 min (and a maximum of 60 min) to allow clot formation, and then centrifuged at 3,000 x g for 10 min at 4°C. After centrifugation, the samples were divided into aliquots in cryotubes and immediately stored at -80°C until use. Samples were handled anonymously according to ethical and legal guidelines at the Verona University Hospital G.B. Rossi.

ELISA assays of ceruloplasmin, galectin-3, MARCKS, and CA19-9 in human serum

ELISA kits were purchased from Abcam Ltd (ceruloplasmin), eBioscience Bender (galectin-3), Sial s.r.l. (MARCKS), and DiaSorin (CA19-9). ELISA were carried out on 120 serum samples (100 from pancreatic cancer and 20 from healthy individuals) using the recommended serum dilution and according to the instructions of the manufacturer. The sensitivity of the ELISA kits for detection of ceruloplasmin, galectin-3, MARCKS, and CA19-9 was 0.6 µg/ml, 0.12 ng/ml, 15.6 pg/ml, and 0.30 U/ml, respectively.

Statistical analysis

The relationship between clinical pathological variables and the level of target proteins was tested using either the Wilcoxon test or Kruskal-Wallis test. A one-tailed Student's t test was performed assuming unequal variances to assess whether the means of healthy normal and PDAC groups were statistically different from each other. The candidates that showed a statistically significant difference (p

< 0.05) were evaluated by a receiver operating characteristic (ROC) curve, and then assessed in comparison to CA19.9. Multiparametric model for combination of ceruloplasmin and CA19-9 was constructed by fitting a logistic regression model on the marker concentrations. All data were processed using GraphPad Prism Software Version 6.0 (La Jolla, CA, USA).

RESULTS

Protein identification and quantification in Panc1 cell and Panc1 CSC conditioned media using iTRAQ

The iTRAQ-labeled CM protein samples of Panc1 cells and Panc1 CSCs were analyzed together with their respective whole cell lysates as shown in **Figure 1**. A total of 2045 proteins with at least 93.8% confidence and an Unused ProteinPilot scores > 1.09 (equating to a global FDR of 1%) were identified, among these a total of 1157 proteins were quantified with a peptide confidence cut-off of 95% (**Supplemental Table 3**). Of these, 608 were identified via a single peptide with a confidence of 99% (**Supplemental Table 4**).

To select Panc1 and Panc1 CSC secreted proteins, the relative abundance of all the proteins in the CM of each sample was compared with that in the respective whole cell lysate. The cut-off for selecting the secreted proteins and those differentially secreted by Panc1 cells and Panc1 CSCs were chosen based on already published data [12]. Briefly, since proteins secreted by a cell should have a higher relative abundance in CM than in cell lysate, i.e. CM/Lysate ratio >1, to have a higher confidence on the secretion nature of the selected proteins, a cut-off >1.5 was used. In addition, only ratios that were reproducible in both biological replicates were taken into account [12]. One hundred and two and 73 proteins were found to have CM/Lysate ratio >1.5 in Panc1 cells and Panc1 CSCs respectively, with an overlap of 63 proteins between the two cell types (**Figure 2A**). The identity of these 112 proteins,

297 together with their respective CM/Lysate ratios, is presented in **Supplemental Table 5**. Among the 112
298 secreted proteins, 72 proteins were differentially secreted by Panc1 cells and Panc1 CSCs when a ratio
299 cut-off >1.5 and <0.667 [12] was applied, 43 with higher accumulation in CM of Panc1 CSCs and 29
300 with higher accumulation in CM of Panc1 cells (**Tables 1** and **2**).
301
302 **Mode of protein secretion**
303 To define if the 112 identified proteins were secreted by the classical or non-classical secretory
304 pathways, we used the SecretomeP 2.0 prediction server. In addition, we used the Exocarta and
305 Vesiclepedia databases, which contain proteins identified in exosomes and extracellular vesicles
306 following non-classical secretory pathways. We found that 30 proteins (27%) were predicted to carry the
307 N-terminal signal peptide that characterizes proteins of the classical secretory pathway, and 82 proteins
308 (73%) were predicted to be secreted by non-classical pathways (**Figure 2B**). In summary, all the 112
309 proteins considered to be secreted using a cut-off CM/Lysate ratio >1.5 in the secretome analysis [12],
310 were confirmed as secreted proteins and have the potential to be addressed to the extracellular space by
311 various mechanisms.
312
313 **Biological functions, pathway analyses, and interaction networks of secreted proteins**
314 To identify altered biological functions and pathways that might play a role in pancreatic cancer
315 epithelial-mesenchymal transition (EMT) and/or metastasis, and to investigate the molecular networks
316 involved, the 112 secreted proteins from Panc1 cells and Panc1 CSCs (indicated in **Figure 2A**, and
317 listed in **Supplemental Table 5**) were analyzed using Ingenuity Pathway Analysis (IPA). In both
318 secretomes, among all the proteins mapped by IPA's knowledgebase, proteins involved in functions such
319 as cell death and survival, cellular movement, cellular growth and proliferation, cell morphology, and

cellular development were significantly over-represented (**Table 3**). In particular, the most relevant associated network functions (score > 40) were "cell death and survival, cellular movement, dermatological diseases and conditions" for Panc1 CSC secretome, and "cell death and survival, cell-to-cell signaling and interaction, connective tissue development and function" and "cell death and survival, cancer, gastrointestinal disease" for Panc1 cell secretome. These network alterations associated with secreted proteins in Panc1 cells and Panc1 CSCs are illustrated in **Supplemental Figure 1**.

We also performed canonical pathway analysis to determine over-represented signalling and metabolic pathways. Twenty-two and 15 canonical pathways were enriched in the Panc1 and Panc1 CSC secretomes, respectively (p-value ≤ 0.001) (**Supplemental Table 6**). The top 6 canonical pathways that included the secreted proteins of Panc1 cells and Panc1 CSCs are shown in **Figure 3**. Interestingly, glycolysis and gluconeogenesis were identified among the top hit list for both secretomes.

Western Blot analysis of selected secreted proteins

In order to validate mass spectrometry-based iTRAQ results, we selected 9 secreted proteins for Western Blot analysis These proteins were selected on the basis of several factors, such as CSCs over-secretion, relevance to PDAC, and novelty. They included vinculin, ceruloplasmin, MARCKS, cathepsin D, glyceraldehyde-3-phosphate deydrogenase (GAPDH), 14-3-3 zeta and epsilon isoforms, galectin-3, and galectin-1. We compared the expression level of secreted proteins by Panc1 cells and Panc1 CSCs in two biological replicates. As shown in **Figure 4,** results from Western Blot analysis were in agreement with iTRAQ data. In particular, Panc1 CSCs were characterized by over-secretion of ceruloplasmin, galectin-3 and MARCKS that appeared to be absent in the secretome of the parental cell line. Similar results were obtained by analyzing ceruloplasmin in the secretome of three further CSC-like cell lines, MiaPaca2, PC1J, and PSN1 [6] (data not shown). Moreover, immunoblot results indicated that

MARCKS was secreted both as intact (~ 80 kDa) and cleaved (~ 40 kDa) forms, and cathepsin D was secreted as procathepsin D (45 kDa) and also as its mature form (30 kDa).

Serum levels of ceruloplasmin, galectin-3, MARCKS, and CA19-9 in PDAC patients

We performed on normal and pathological human sera an immunoassay-based analysis of highly secreted CSCs proteins and evaluated the potential of this determination to detect PDAC patients. Particularly, we focused our attention on the three proteins more secreted by Panc1 CSCs as compared to Panc1 cells (i.e. ceruloplasmin, galectin-3, and MARCKS), as well as on CA19-9, and verified their association with gender, age, histological grade, overall tumour stage, or TNM classification of PDAC. We found that serum levels of galectin-3 correlate with patient age, while serum levels of MARCKS correlate with patient gender (**Supplemental Table 7**).

We tested and quantified the presence of ceruloplasmin, galectin-3, and MARCKS in PDAC patient sera by using commercially available ELISA (**Figure 5**). The analysis of serum samples (100 cancer versus 20 healthy) showed significant higher levels ($p < 0.01$) of ceruloplasmin in PDAC (mean = 73.15 µg/ml, median = 63.50 µg/ml) in comparison to controls (mean = 57.13 µg/ml, median = 53.54 µg/ml). In addition we found that serum levels of ceruloplasmin were significantly elevated in patients with PDAC at the early IIB stage ($p < 0.01$) and at stage III ($p < 0.05$) (**Figure 5**) compared to those in healthy control. In the same samples, MARCKS also showed significant ($p < 0.05$) elevation in cancer (mean = 149.45 pg/ml, median = 107.75 pg/ml) as compared to controls (mean = 110.89 pg/ml, median = 94.69 pg/ml), but there was no significant difference among patients with different PDAC stages (**Figure 5)**. As concerning galectin-3 similar levels were present in patients (mean = 4.43 ng/ml, median = 4.10 ng/ml) and controls (mean = 4.61 ng/ml, median = 4.18 ng/ml) without significant difference among different stages (**Figure 5**). Serum levels of CA 19-9, a currently used serum PDAC biomarker,

were significantly higher ($p < 0.05$) in PDAC patients (mean = 1283.36 U/ml, median = 170.00 U/ml) than in healthy controls (mean = 8.76 U/ml, median = 6.50 U/ml). In addition CA19-9 also shown significant elevation in patients with PDAC stage IIB ($p < 0.001$), stage III ($p < 0.05$), and stage IV ($p < 0.05$) (**Figure 5**).

Receiver operating characteristic (ROC) curve analysis was carried out to evaluate the individual performance of ceruloplasmin, MARCKS and CA19-9 (**Figure 6**). This analysis showed lower AUCs for ceruloplasmin (AUC = 0.65; 95% CI: 0.54 – 0.76) and MARCKS (AUC = 0.56; 95% CI: 0.43 – 0.70) in discriminating healthy controls from PDAC patients, in comparison with CA19-9 (AUC = 0.90, 95% CI: 0.85 – 0.96). In particular, the AUC obtained for MARCKS indicates that it has virtually no discriminating power. Ceruloplasmin (cut-off = 60.75 µg/ml) has lower sensitivity (55%) than CA19-9 (77%) in diagnosing PDAC. However, it is interesting to note that among the 25 patients with clinically low CA19-9 (< 37 U/ml), 14 (56%) were positive for ceruloplasmin (**Supplemental Figure 2**).

Most importantly, a logistic regression model showed that the diagnostic capacity of the combination of ceruloplasmin and CA19-9 (AUC = 0.93; 95% CI: 0.88 – 0.97) was more discriminatory than CA19-9 alone (AUC = 0.90; 95% CI: 0.85 – 0.96). In addition, the combined predictor using information from both ceruloplasmin and CA19-9 showed increased sensitivity (83%) than CA19-9 alone (77%).

DISCUSSION

The ability to identify and isolate CSCs in various tumour models has led to the possibility to study the mechanisms by which CSCs can contribute to tumour initiation as well as continued tumour progression. Up to now, a deep comprehension of CSC biology, and in particular that of pancreatic CSCs, is lacking. In the present study, a comparative secretome approach was taken to dissect the

differences in protein level between pancreatic cancer and pancreatic cancer stem cells. Secreted proteins are key mediators in cell-cell interactions and influence the cross talk with the surrounding tissues. Strong evidences support the idea that crucial cellular functions, such as proliferation, differentiation, communication, and migration, are strictly regulated by proteins secreted by the cells [20]. Thus, the investigation of CSC secretome is extremely important to clarify the deregulated pathways involved in pancreatic cancer, but also to suggest possible new diagnostic markers. For this purpose we have investigated the Panc-1 CSCs model that was previously characterized [6]. In particular, we have compared the secretome of CSCs with that of the parental cell line and we have identified the differentially secreted proteins, by applying a shotgun proteomic approach based on iTRAQ technology. Some of the most interesting differentially secreted proteins have also been validated by immunoblotting. Some of the Panc-1 CSCs over-secreted proteins identified in this study have already been reported in previous publications. In particular, 14-3-3 protein epsilon, 14-3-3 protein zeta/delta, annexin A5, glutathione S-transferase omega-1, plasminogen activator inhibitor 1, protein disulfide-isomerase, and superoxide dismutase [Cu-Zn] were reported by Mateo et al. [11] as over-secreted by prostate CSCs and WD repeat domain 1 was reported by Emmink et al. [10] as over-secreted by colon CSCs.

Deregulated pathways of the Panc1 CSC secretome

The identified secreted proteins were overlaid with IPA-curated canonical pathways to explore possible metabolic and cell signalling pathways that are over-represented by the experimentally determined proteins. Despite some of the aberrant signalling pathways have been already identified in CSCs, like Hedgehog, Notch, Wnt/β-catenin, BMI1, PI3K/AKT, and Nodal/Activin [21, 22], and several

markers have been used to define CSCs, the signalling pathways regulating these events and markers remain not fully determined.

Our analysis has shown that glycolysis and gluconeogenesis are the two most significant pathways in which the secreted proteins of both Panc1 cells and Panc1 CSCs are implicated (**Figure 3**). It has been largely demonstrated that the high glycolytic activity of PDAC and the consequent alteration of the glucose-connected metabolic pathways contribute to the progression and dissemination of the disease [23]. In addition, our findings further confirm that glycolytic and gluconeogenesis enzymes can be secreted by cells. Notably, it has been demonstrated that these enzymes perform non enzymatic, but rather structural or regulatory functions at the extracellular localization. For instance, in tumour cells the surface exposition of alpha-enolase (ENO1) acts as a plasminogen receptor, mediating plasmin activation, extracellular matrix degradation, and supporting anaerobic proliferation [24].

IPA analysis has also shown, among the significant pathways ($p < 0.001$) characterizing only the CSC secretome, the pentose phosphate (PP) pathway (non-oxidative branch), glioma invasiveness signalling, myc-mediated apoptosis signalling, ERK5 signalling, and remodelling of epithelial adherens junctions (**Supplemental Table 6**).

The PP pathway plays a major role in stem cell biology, indeed, CSCs have been shown to possess a protective metabolic phenotype, mainly based on glycolysis and PP pathway, to scavenge reactive oxygen species (ROS) generated by oxidative metabolism [25]. It remains unclear why the PP enzymes are secreted and which function they have at the extracellular level. In particular, our study has shown that the CSC secretome is characterized by the presence of the PP enzyme transaldolase (> 1.93 in CSC secretome compared to Panc1 secretome), which catalyses a non-oxidative phase reaction. Currently, the extracellular function of transaldolase has been clarified only for Bifidobacterium, where it has a role in mucin adhesion and cell aggregation [26]. Interestingly, it has been reported that mucins

play a key role in PDAC by enhancing tumourigenicity, invasiveness, metastasis and drug resistance [27].

The glioma invasiveness signalling involves secreted proteins including 72 kDa type IV collagenase (MMP2), urokinase-type plasminogen activator (UROK/PLAU), and metalloproteinase inhibitor 2 (TIMP2). These three proteins, however, are not exclusive of the CSC secretome, but were also identified in the secretome of the Panc1 parental cell line (see **Supplemental Table 5**). Matrix metalloproteinase family plays a critical role in tumour cell invasion and metastasis. In particular, MMP2 secretion and activation, and the consequent increased tumour invasiveness, depend on ROS generation, which occurs after hypoxia-reoxygenation of Panc1 cells [28]. Recently, it has also been demonstrated that reoxygenation from chronic hypoxia promotes metastatic processes in pancreatic cancer through the Hedgehog signalling, a peculiar pathway of pancreatic CSCs [29]. Moreover, stimulation of Panc1 cells with bone morphogenetic proteins (BMP2) induces MMP2 secretion and activation, in association with decreased expression of E-cadherin (an invasion suppressor), and leads to EMT and cell invasion [30]. TIMPs are naturally occurring inhibitors of MMPs that inhibit the MMP activity and hence restrict breakdown of ECM, maintains connective tissue integrity, thus slow down carcinogenesis, tumour invasion and metastasis. Disturbance in balance of MMPs and TIMPs is found in associated with various pathologic conditions including cancer. Interestingly, sequence variants of TIMP2 (TIMP2c.418G>C variants), are associated with the development of tumour growth and progression [31], this may be because of low promoter activity for TIMP-2 expression, resulting in slow inhibition of MMPs, leading to inflammatory microenvironment and carcinogenesis. Also UROK is involved in the degradation of the extracellular matrix, tumour cell migration and proliferation. It converts plasminogen to plasmin, which in turn can degrade a wide variety of extracellular matrix components and enable the tumour cells to penetrate the basement membrane. The induced expression in

PDAC of this protease depends on the activation of the EGFR/NF-κB axis, which is mediated by the oncogene K-Ras and loss of Smad4 [32].

It is interesting to note that two other pathways characteristic of CSC secretome, i.e. myc-mediated apoptosis signalling and ERK5 signalling, involve the 14-3-3 proteins. Recently, it has been proved that 14-3-3ζ proteins are secreted, together with β-catenin, via extracellular vesicles to activate the oncogenic Wnt pathway [33], which is a peculiar pathways of CSCs. It is known that as a result of uptake of 14-3-3ζ containing-exosomes, the oncogenic Wnt pathway becomes activate also in surrounding cells. Moreover, it has been demonstrated that 14-3-3ζ protein is involved in EMT in lung [34], as well as in breast [35] cancer, while both isoforms 14-3-3ε and ζ are involved in EMT in hepatocellular carcinoma [36].

Another pathway characteristic of the CSC secretome is the "remodelling of epithelial adherens junctions" which comprises nucleoside diphosphate kinase A (NDKA/NME1), vinculin (VINC/VCL), and alpha-actinin-4 (ACTN4). Vinculin is a highly conserved actin-binding protein that is localized in integrin-mediated focal adhesion complexes and is indispensable for hematopoietic stem cell repopulation [37]. In particular, vinculin has a key role in the molecular mechanisms that sense extracellular matrix stiffness, which is known to direct the lineage specification of stem cells and to affect cancer progression [38]. Alpha-actinin-4 is a cell motility–associated actin-binding protein that has a tumour-promoting potential in PDAC [39]. Interestingly, it forms a complex with β-catenin in the absence of E-cadherin and mediates cancer invasion and metastasis [40].

Evaluation of the potential use as biomarkers of ceruloplasmin, galectin-3, and MARCKS

Among the identified proteins, we selected ceruloplasmin, galectin-3 and MARCKS for further evaluation of their clinical relevance in PDAC.

Ceruloplasmin is the major copper-carrying protein in the blood, with both anti- and pro-oxidant activities. It can be expressed as a membrane glycosylphosphatidylinositol-anchored protein, or can be secreted by a classical mechanism involving a single peptide [41]. Ceruloplasmin levels are reported to be increased in sera of patients with various acute inflammatory conditions, including injury, malignancy, cardiovascular disease, and infection [42]. Also in PDAC patients ceruloplasmin appears to be increased as detected by a liquid ESI-MS analysis [43]. It has been suggested that the increased presence of ceruloplasmin in the sera of pancreatic cancer patients is consistent with the overall hypothesis that pancreatic cancer has an inflammatory disease component. Tobacco smoke and alcohol are in fact known risk agents for pancreatic cancer.

Here, we show that ceruloplasmin is strongly increased in CSCs secretome (>15.93) compared to the parental cell line. Accordingly, this protein has been found enriched also in secretomes of other CSCs, in particular malignant glioma stem-like cells, where its production is regulated by hyaluronan, which interacts with CD44 receptors, also present on pancreatic CSCs [44]. Ceruloplasmin acts as a ferroxidase, an enzyme essential for normal iron homeostasis, which plays a critical role in EMT [45]. In addition, concentration of ceruloplasmin was significantly higher in the ascites fluids of chemoresistant ovarian cancer patients [46]. In parallel, CSC over-secretion of ceruloplasmin detected in our samples may correlate with the known resistance to gemcitabine chemotherapy in pancreatic cancer. Indeed, the observation that gemcitabine induces apoptosis by raising intracellular ROS levels let to hypothesis that secreted ceruloplasmin may lead to chemoresistance by decreasing ROS levels. We showed that ceruloplasmin could discriminate controls from PDAC patients and, remarkably, also patients at the early stages (**Figure 5**).

It should be pointed out that differentially expressed or secreted candidates are sometimes a result of the generic acute phase reactions, which should not be misinterpreted as promising markers. Hence, as a

general rule, the identification of a combination of biomarkers is considered to be much more effective for detection of specific cancer. To this end, we investigated the performance of ceruloplasmin in combination with CA19-9. We found that the combination of CA19- 9 and ceruloplasmin improve the AUC of CA19-9 alone (**Figure 6**) and that ceruloplasmin levels were higher than controls in more than 50% of patients negative for CA19-9. These findings suggest that ceruloplasmin might prove to be a valuable complementary biomarker for CA19-9.

Galectin-3 is a 30 kDa galactoside-binding protein expressed in several cell types and is involved in a broad range of physiological and pathological processes, especially in regulating cancer cell activities [47]. Indeed, galectin-3 has been widely demonstrated to be involved in malignant cell transformation, tumour growth, *anoikis* resistance, apoptosis inhibition, chemoresistance, angiogenesis, cell adhesion, cell motility, and cell invasion [48]. The latter four events are important steps of the metastatic process, in which secreted galectin-3 plays a key role in both tumour and stromal cells of the tumour microenvironment [49]. Here, we show that galectin-3 is over-secreted by CSCs (>12.59 compared to parental cells). Up to now, the non-classical mechanism for galectin-3 secretion is not clear, but data obtained so far suggest that galectin-3 is secreted via exosomes [50]. This protein has already been found as secreted by other stem cells, for example mesenchymal stem cells to induce suppression of T-cell proliferation [51], consistent with its involvement in tumour-immune-escape mechanisms. Interestingly, galectin-3 is also implicated in the pathogenesis of PDAC [52]. In a recent study, it has been demonstrated that galectin-3 is directly associated with the oncogene K-Ras and contributes to its activation in pancreatic cancer cells [53]. Furthermore, it has been shown that transient silencing of galectin-3 suppresses PDAC malignant behaviour [54], suggesting a functional role in PDAC tumour progression and invasion. The clinical significance of serum galectin-3 in pancreatic carcinoma is currently not fully clarified. The available data are conflicting: it has been demonstrated to be higher in

serum of PDAC patients as compared to controls [55], although a separate study showed it to be unchanged between these groups [56]. For this reason, given that galectin-3 was highly elevated in the secretome of Panc1 CSCs, we tested its levels in our screening set of serum samples by ELISA and found that there was no significant increase in levels in pancreatic cancer sera *versus* controls (**Figure 5**).

The third most abundant CSC secreted protein is MARCKS. MARCKS, a major phosphorylation target for protein kinase C, is typically membrane-bound through a lipid anchor at the N-terminus, and a polybasic domain in the middle, however, it has also already been found in cell secretome of colorectal cancer metastatic cells [57]. MARCKS is a key regulatory molecule controlling mucus granule secretion by airway epithelial cells, as well as directed migration of leukocytes, fibroblasts and mesenchymal stem cells [58]. Recently, it has been demonstrated that a peptide that inhibits MARCKS function reduces lung cancer metastasis [59]. However, MARCKS has been reported in glioma and melanoma cells to possess not only a pro-metastatic [60, 61] but also a growth suppressor activity [62, 63]. Interestingly, MARCKS was found to have a strikingly higher expressed transcript in pancreatic cancer cell lines with a mutated K-Ras (Panc1, Capan-2, and MiaPaCa2) in comparison to pancreatic cancer cell lines with the wild-type K-Ras gene (Hs766T and BxPC-3) [64]. Accordingly, a severe decrease in MARCKS expression has been shown to correlate with Ras reversion [65]. Our results indicate that MARCKS is over-secreted (> 10.79) by CSCs relative to parental cells. However, even if the verification analysis performed on the sera showed that this marker discriminates between controls and PDAC patients (**Figure 5**), the ROC curve indicated that it does not have diagnostic accuracy (**Figure 6**).

In conclusion, our Panc1 and Panc1 CSCs secretome analysis revealed a large number of secreted proteins, which participate in pathological conditions including cancer differentiation, invasion and metastasis. The identified proteins may serve as a valuable pool of proteins from which cancer

biomarkers and or therapeutic targets can be identified. Among the highly CSC secreted proteins, ceruloplasmin looks promising and further validation in bigger cohorts of patients and healthy controls is hopeful.

REFERENCES

[1] Saif MW. Pancreatic neoplasm in 2011: an update. JOP 2011; 12: 316-21.
[2] Rhim AD, Mirek ET, Aiello NM, Maitra A, Bailey JM, McAllister F, et al. EMT and dissemination precede pancreatic tumor formation. Cell 2012; 148: 349-61.
[3] Lee CJ, Dosch J, and Simeone DM. Pancreatic cancer stem cells. J Clin Oncol 2008; 26: 2806-12.
[4] Li C, Heidt DG, Dalerba P, Burant CF, Zhang L, Adsay V, et al. Identification of pancreatic cancer stem cells. Cancer Res 2007; 67: 1030-7.
[5] Kondo T. Stem cell-like cancer cells in cancer cell lines. Cancer Biomark 2007; 3: 245-50.
[6] Dalla Pozza E, Dando I, Biondani G, Brandi J, Costanzo C, Zoratti E, et al. Pancreatic ductal adenocarcinoma cell lines display a plastic ability to bidirectionally convert into cancer stem cells. Int J Oncol 2015; 46: 1099-108.
[7] Dai L, Li C, Shedden KA, Lee CJ, Quoc H, Simeone DM, et al. Quantitative proteomic profiling studies of pancreatic cancer stem cells. J Proteome Res 2010; 9: 3394-402.
[8] Zhu J, Nie S, Wu J, and Lubman DM. Target proteomic profiling of frozen pancreatic CD24+ adenocarcinoma tissues by immuno-laser capture microdissection and nano-LC-MS/MS. J Proteome Res 2013; 12: 2791-804.
[9] Zhu J, He J, Liu Y, Simeone DM, and Lubman DM. Identification of glycoprotein markers for pancreatic cancer CD24+CD44+ stem-like cells using nano-LC-MS/MS and tissue microarray. J Proteome Res 2012; 11: 2272-81.
[10] Emmink BL, Verheem A, Van Houdt WJ, Steller EJ, Govaert KM, Pham TV, et al. The secretome of colon cancer stem cells contains drug-metabolizing enzymes. J Proteomics 2013; 91: 84-96.
[11] Mateo F, Meca-Cortes O, Celia-Terrassa T, Fernandez Y, Abasolo I, Sanchez-Cid L, et al. SPARC mediates metastatic cooperation between CSC and non-CSC prostate cancer cell subpopulations. Mol Cancer 2014; 13: 237.
[12] Loei H, Tan HT, Lim TK, Lim KH, So JB, Yeoh KG, et al. Mining the gastric cancer secretome: identification of GRN as a potential diagnostic marker for early gastric cancer. J Proteome Res 2012; 11: 1759-72.
[13] Shilov IV, Seymour SL, Patel AA, Loboda A, Tang WH, Keating SP, et al. The Paragon Algorithm, a next generation search engine that uses sequence temperature values and feature probabilities to identify peptides from tandem mass spectra. Mol Cell Proteomics 2007; 6: 1638-55.
[14] Tang WH, Shilov IV, and Seymour SL. Nonlinear fitting method for determining local false discovery rates from decoy database searches. J Proteome Res 2008; 7: 3661-7.
[15] Bendtsen JD, Jensen LJ, Blom N, Von Heijne G, and Brunak S. Feature-based prediction of non-classical and leaderless protein secretion. Protein Eng Des Sel 2004; 17: 349-56.
[16] Simpson RJ, Kalra H, and Mathivanan S. ExoCarta as a resource for exosomal research. J Extracell Vesicles 2012; 1.
[17] Kalra H, Simpson RJ, Ji H, Aikawa E, Altevogt P, Askenase P, et al. Vesiclepedia: a compendium for extracellular vesicles with continuous community annotation. PLoS Biol 2012; 10: e1001450.
[18] Karagiannis GS, Pavlou MP, Saraon P, Musrap N, Xie A, Batruch I, et al. In-depth proteomic delineation of the colorectal cancer exoproteome: Mechanistic insight and identification of potential biomarkers. J Proteomics 2014; 103: 121-36.
[19] Jenkinson C, Elliott V, Menon U, Apostolidou S, Fourkala OE, Gentry-Maharaj A, et al. Evaluation in pre-diagnosis samples discounts ICAM-1 and TIMP-1 as biomarkers for earlier diagnosis of pancreatic cancer. J Proteomics 2015; 113: 400-2.
[20] Makridakis M, Roubelakis MG, and Vlahou A. Stem cells: insights into the secretome. Biochim Biophys Acta 2013; 1834: 2380-4.
[21] Abel EV, and Simeone DM. Biology and clinical applications of pancreatic cancer stem cells. Gastroenterology 2013; 144: 1241-8.
[22] Quan M, Wang P, Cui J, Gao Y, and Xie K. The roles of FOXM1 in pancreatic stem cells and carcinogenesis. Mol Cancer 2013; 12: 159.

[23] Guillaumond F, Iovanna JL, and Vasseur S. Pancreatic tumor cell metabolism: focus on glycolysis and its connected metabolic pathways. Arch Biochem Biophys 2014; 545: 69-73.
[24] Capello M, Ferri-Borgogno S, Cappello P, and Novelli F. alpha-Enolase: a promising therapeutic and diagnostic tumor target. FEBS J 2011; 278: 1064-74.
[25] Perales-Clemente E, Folmes CD, and Terzic A. Metabolic regulation of redox status in stem cells. Antioxid Redox Signal 2014; 21: 1648-59.
[26] Gonzalez-Rodriguez I, Sanchez B, Ruiz L, Turroni F, Ventura M, Ruas-Madiedo P, et al. Role of extracellular transaldolase from Bifidobacterium bifidum in mucin adhesion and aggregation. Appl Environ Microbiol 2012; 78: 3992-8.
[27] Kaur S, Kumar S, Momi N, Sasson AR, and Batra SK. Mucins in pancreatic cancer and its microenvironment. Nat Rev Gastroenterol Hepatol 2013; 10: 607-20.
[28] Binker MG, Binker-Cosen AA, Richards D, Gaisano HY, de Cosen RH, and Cosen-Binker LI. Hypoxia-reoxygenation increase invasiveness of PANC-1 cells through Rac1/MMP-2. Biochem Biophys Res Commun 2010; 393: 371-6.
[29] Morifuji Y, Onishi H, Iwasaki H, Imaizumi A, Nakano K, Tanaka M, et al. Reoxygenation from chronic hypoxia promotes metastatic processes in pancreatic cancer through the Hedgehog signaling. Cancer Sci 2014; 105: 324-33.
[30] Liu J, Ben QW, Yao WY, Zhang JJ, Chen DF, He XY, et al. BMP2 induces PANC-1 cell invasion by MMP-2 overexpression through ROS and ERK. Front Biosci (Landmark Ed) 2012; 17: 2541-9.
[31] Sharma KL, Misra S, Kumar A, and Mittal B. Higher risk of matrix metalloproteinase (MMP-2, 7, 9) and tissue inhibitor of metalloproteinase (TIMP-2) genetic variants to gallbladder cancer. Liver Int 2012; 32: 1278-86.
[32] Bera A, Zhao S, Cao L, Chiao PJ, and Freeman JW. Oncogenic K-Ras and loss of Smad4 mediate invasion by activating an EGFR/NF-kappaB Axis that induces expression of MMP9 and uPA in human pancreas progenitor cells. PLoS One 2013; 8: e82282.
[33] Dovrat S, Caspi M, Zilberberg A, Lahav L, Firsow A, Gur H, et al. 14-3-3 and beta-catenin are secreted on extracellular vesicles to activate the oncogenic Wnt pathway. Mol Oncol 2014; 8: 894-911.
[34] Chen CH, Chuang SM, Yang MF, Liao JW, Yu SL, and Chen JJ. A novel function of YWHAZ/beta-catenin axis in promoting epithelial-mesenchymal transition and lung cancer metastasis. Mol Cancer Res 2012; 10: 1319-31.
[35] Lu J, Guo H, Treekitkarnmongkol W, Li P, Zhang J, Shi B, et al. 14-3-3zeta Cooperates with ErbB2 to promote ductal carcinoma in situ progression to invasive breast cancer by inducing epithelial-mesenchymal transition. Cancer Cell 2009; 16: 195-207.
[36] Liu TA, Jan YJ, Ko BS, Liang SM, Chen SC, Wang J, et al. 14-3-3epsilon overexpression contributes to epithelial-mesenchymal transition of hepatocellular carcinoma. PLoS One 2013; 8: e57968.
[37] Ohmori T, Kashiwakura Y, Ishiwata A, Madoiwa S, Mimuro J, Furukawa Y, et al. Vinculin is indispensable for repopulation by hematopoietic stem cells, independent of integrin function. J Biol Chem 2010; 285: 31763-73.
[38] Yamashita H, Ichikawa T, Matsuyama D, Kimura Y, Ueda K, Craig SW, et al. The role of the interaction of the vinculin proline-rich linker region with vinexin alpha in sensing the stiffness of the extracellular matrix. J Cell Sci 2014; 127: 1875-86.
[39] Welsch T, Keleg S, Bergmann F, Bauer S, Hinz U, and Schmidt J. Actinin-4 expression in primary and metastasized pancreatic ductal adenocarcinoma. Pancreas 2009; 38: 968-76.
[40] Hayashida Y, Honda K, Idogawa M, Ino Y, Ono M, Tsuchida A, et al. E-cadherin regulates the association between beta-catenin and actinin-4. Cancer Res 2005; 65: 8836-45.
[41] Koschinsky ML, Funk WD, van Oost BA, and MacGillivray RT. Complete cDNA sequence of human preceruloplasmin. Proc Natl Acad Sci U S A 1986; 83: 5086-90.
[42] Healy J, and Tipton K. Ceruloplasmin and what it might do. J Neural Transm 2007; 114: 777-81.
[43] Hanas JS, Hocker JR, Cheung JY, Larabee JL, Lerner MR, Lightfoot SA, et al. Biomarker identification in human pancreatic cancer sera. Pancreas 2008; 36: 61-9.

[44] Tye SL, Gilg AG, Tolliver LB, Wheeler WG, Toole BP, and Maria BL. Hyaluronan regulates ceruloplasmin production by gliomas and their treatment-resistant multipotent progenitors. J Child Neurol 2008; 23: 1221-30.
[45] Zhang KH, Tian HY, Gao X, Lei WW, Hu Y, Wang DM, et al. Ferritin heavy chain-mediated iron homeostasis and subsequent increased reactive oxygen species production are essential for epithelial-mesenchymal transition. Cancer Res 2009; 69: 5340-8.
[46] Huang H, Li Y, Liu J, Zheng M, Feng Y, Hu K, et al. Screening and identification of biomarkers in ascites related to intrinsic chemoresistance of serous epithelial ovarian cancers. PLoS One 2012; 7: e51256.
[47] Fortuna-Costa A, Gomes AM, Kozlowski EO, Stelling MP, and Pavao MS. Extracellular galectin-3 in tumor progression and metastasis. Front Oncol 2014; 4: 138.
[48] Zhang D, Chen ZG, Liu SH, Dong ZQ, Dalin M, Bao SS, et al. Galectin-3 gene silencing inhibits migration and invasion of human tongue cancer cells in vitro via downregulating beta-catenin. Acta Pharmacol Sin 2013; 34: 176-84.
[49] Yamamoto-Sugitani M, Kuroda J, Ashihara E, Nagoshi H, Kobayashi T, Matsumoto Y, et al. Galectin-3 (Gal-3) induced by leukemia microenvironment promotes drug resistance and bone marrow lodgment in chronic myelogenous leukemia. Proc Natl Acad Sci U S A 2011; 108: 17468-73.
[50] Mehul B, and Hughes RC. Plasma membrane targetting, vesicular budding and release of galectin 3 from the cytoplasm of mammalian cells during secretion. J Cell Sci 1997; 110 (Pt 10): 1169-78.
[51] Sioud M, Mobergslien A, Boudabous A, and Floisand Y. Evidence for the involvement of galectin-3 in mesenchymal stem cell suppression of allogeneic T-cell proliferation. Scand J Immunol 2010; 71: 267-74.
[52] Jiang K, Lawson D, Cohen C, and Siddiqui MT. Galectin-3 and PTEN expression in pancreatic ductal adenocarcinoma, pancreatic neuroendocrine neoplasms and gastrointestinal tumors on fine-needle aspiration cytology. Acta Cytol 2014; 58: 281-7.
[53] Song S, Ji B, Ramachandran V, Wang H, Hafley M, Logsdon C, et al. Overexpressed galectin-3 in pancreatic cancer induces cell proliferation and invasion by binding Ras and activating Ras signaling. PLoS One 2012; 7: e42699.
[54] Kobayashi T, Shimura T, Yajima T, Kubo N, Araki K, Tsutsumi S, et al. Transient gene silencing of galectin-3 suppresses pancreatic cancer cell migration and invasion through degradation of beta-catenin. Int J Cancer 2011; 129: 2775-86.
[55] Xie L, Ni WK, Chen XD, Xiao MB, Chen BY, He S, et al. The expressions and clinical significances of tissue and serum galectin-3 in pancreatic carcinoma. J Cancer Res Clin Oncol 2012; 138: 1035-43.
[56] Gaida MM, Bach ST, Gunther F, Baseras B, Tschaharganeh DF, Welsch T, et al. Expression of galectin-3 in pancreatic ductal adenocarcinoma. Pathol Oncol Res 2012; 18: 299-307.
[57] Barderas R, Mendes M, Torres S, Bartolome RA, Lopez-Lucendo M, Villar-Vazquez R, et al. In-depth characterization of the secretome of colorectal cancer metastatic cells identifies key proteins in cell adhesion, migration, and invasion. Mol Cell Proteomics 2013; 12: 1602-20.
[58] Miller JD, Lankford SM, Adler KB, and Brody AR. Mesenchymal stem cells require MARCKS protein for directed chemotaxis in vitro. Am J Respir Cell Mol Biol 2010; 43: 253-8.
[59] Chen CH, Thai P, Yoneda K, Adler KB, Yang PC, and Wu R. A peptide that inhibits function of Myristoylated Alanine-Rich C Kinase Substrate (MARCKS) reduces lung cancer metastasis. Oncogene 2014; 33: 3696-706.
[60] Chen X, and Rotenberg SA. PhosphoMARCKS drives motility of mouse melanoma cells. Cell Signal 2010; 22: 1097-103.
[61] Micallef J, Taccone M, Mukherjee J, Croul S, Busby J, Moran MF, et al. Epidermal growth factor receptor variant III-induced glioma invasion is mediated through myristoylated alanine-rich protein kinase C substrate overexpression. Cancer Res 2009; 69: 7548-56.
[62] Jarboe JS, Anderson JC, Duarte CW, Mehta T, Nowsheen S, Hicks PH, et al. MARCKS regulates growth and radiation sensitivity and is a novel prognostic factor for glioma. Clin Cancer Res 2012; 18: 3030-41.
[63] Brooks G, Brooks SF, and Goss MW. MARCKS functions as a novel growth suppressor in cells of melanocyte origin. Carcinogenesis 1996; 17: 683-9.

694 [64] Gardner-Thorpe J, Ito H, Ashley SW, and Whang EE. Differential display of expressed genes in pancreatic
695 cancer cells. Biochem Biophys Res Commun 2002; 293: 391-5.
696 [65] Wojtaszek PA, Stumpo DJ, Blackshear PJ, and Macara IG. Severely decreased MARCKS expression correlates
697 with ras reversion but not with mitogenic responsiveness. Oncogene 1993; 8: 755-60.
698
699

700 **Acknowledgments:** We thank Dr. Salvagno Gianluca for technical assistance with CA19-9 ELISA

701 assays. This work was supported by AIRC-Fondazione CariPaRo, Padova, Italy; AIRC 5 per mille grant

702 n. 12182, Italy and the NIHR Liverpool Pancreas Biomedical Research Unit. JB received a travel

703 Fellowship from the European Pancreatic Club.

704

705 **Competing financial interests:** The authors declare no competing financial interests.

706

Figure Legends

Figure 1. Schematic representation of the experimental design for iTRAQ labeling showing biological replicates**.** Samples were trypsinized prior to iTRAQ labeling, and the labeled peptides were then mixed, separated by 2D-LC, and identified by MS/MS. Database search and iTRAQ analysis were performed using the ProteinPilot software (Version 4.2) from AB SCIEX.

Figure 2. Secretome of Panc1 cells and Panc1 CSCs. (A) Venn diagram showing the number of proteins with CM/Lysate ratio >1.5 that were identified in Panc1 cells and Panc1 CSCs. The intersection indicates the number of proteins secreted by both cell lines. (B) SecretomeP prediction of the proteins with CM/Lysate ratio >1.5. Amino acid sequences of these proteins were retrieved from Uniprot and imported into the SecretomeP 2.0 server for prediction of mode of secretion.

Figure 3. The top 6 signalling pathways that significantly ($p < 0.001$) characterize the secretome of (A) Panc1 (B) and Panc1 CSCs data sets. Bioinformatics analyses were performed using IPA software. The pathways are ranked by p value, which is a measure of significance of the changes induced in the secretome. The threshold corresponds to the significance at 95% confidence. The ratio is calculated as follows: the number of molecules in a given pathway that meet cut-off criteria, divided by total number of molecules that make up that pathway.

Figure 4. Confirmation of iTRAQ results by Western blot. Proteins from conditioned media were resolved in 10-20% SDS-PAGE gels, transferred onto PVDF membranes, and probed with specific antibodies against the indicated targets. Ponceau S stained blot is shown to demonstrate equal loading.

Figure 5. Ceruloplasmin, MARCKS, galectin-3, and CA19-9 concentration blood sera. Analysis of serum concentrations were determined in serum samples of PDAC patients (n = 100) and healthy controls (n = 20). The levels of the four proteins were measured in patients at different TNM stages. As regarding ceruloplasmin there were significant difference between controls and the early IIB stage ($p < 0.01$), and stage III ($p < 0.05$). For CA19-9 there were significant difference between controls and the early IIB stage ($p < 0.001$), stage III ($p < 0.05$), and stage IV ($p < 0.05$). For MARCKS and galectin-3 there were no significant differences among different stages. Data are represented in dot plots, horizontal bar represents the median of the ELISA value data set. * = p value < 0.05; ** = p value < 0.01; *** = p value <0.001.

Figure 6. Receiver Operating Characteristic curve analysis for Ceruloplasmin, MARCKS and CA19.9. AUC (area under curve) is given at 95% confidence intervals (CI). AUC of ceruloplasmin, MARCKS, and CA19.9 is depicted individually in this sample set of 20 controls and 100 PDAC. The combination of ceruloplasmin with CA19.9 shows improved AUC to CA19.9 alone.

Table 1. Secreted proteins with higher abundance in the CM of Panc1 CSCs compared to Panc1 cells.

Name	Unused	Total	% Seq Coverage (95)	UniProt/Swiss Prot Accession	Peptides (> 93.8%)	Peptides used for quant	Average CM CSCs / Panc1 (>1.5) [a]	sd	SecretomeP [b]	ExoCarta [c]	Vesiclepedia [d]
Ceruloplasmin	9.1	9.29	7.32	P00450	6	4	15.93	3.26	SP		
Galectin-3	13.95	13.95	27.20	P17931	7	36	12.59	1.44	NC		
Myristoylated alanine-rich C-kinase substrate	26.44	26.48	56.02	P29966	15	49	10.79	3.04		present	
Transaldolase	17.08	18.56	24.04	P37837	9	35	6.10	1.93		present	
Galectin-1	19.37	19.4	62.96	P09382	11	102	5.63	0.26		present	
Insulin-like growth factor-binding protein 7	8.03	8.03	19.50	Q16270	4	11	5.26	0.59	SP		
Glyceraldehyde-3-phosphate dehydrogenase	49.39	49.39	62.09	P04406	26	140	5.18	0.51		present	
Cytosolic non-specific dipeptidase	13.01	13.06	15.37	Q96KP4	7	9	4.95	1.94		present	
Tyrosine--tRNA ligase, cytoplasmic	25.09	26.14	25.00	P54577	13	10	4.65	1.07			present
Phosphoglucomutase-1	23.02	23.37	28.83	P36871	12	6	4.52	2.84		present	
Non-histone chromosomal protein HMG-14	10.53	10.53	51.00	P05114	6	23	4.36	2.09			present
Chloride intracellular channel protein 1	20.77	21.39	63.49	O00299	11	35	4.24	1.47		present	
Glutathione S-transferase P	16.15	17.03	52.38	P09211	8	22	4.00	1.86	NC		
Lactoylglutathione lyase	5.8	5.81	14.67	Q04760	4	8	3.95	1.85		present	
Vinculin	88.07	89.75	42.24	P18206	46	150	3.92	0.36		present	
Protein DJ-1	22.7	24.19	59.79	Q99497	10	31	3.35	0.54		present	
Thioredoxin	4.08	4.11	20.95	P10599	2	18	3.03	0.55		present	
14-3-3 protein epsilon	15.85	22.52	55.29	P62258	9	48	3.03	0.08		present	
60S acidic ribosomal protein P2	22.12	22.58	76.52	P05387	13	45	2.82	0.66		present	
Cathepsin D	31.44	33.44	44.66	P07339	19	74	2.76	1.12	SP		
L-lactate dehydrogenase B chain	21.34	27.05	44.31	P07195	14	81	2.73	0.17	NC		
T-complex protein 1 subunit beta	40.95	43.05	52.34	P78371	21	55	2.69	0.88	NC		
Fructose-bisphosphate aldolase A	51.66	51.66	67.58	P04075	29	94	2.58	0.05		present	
Glutathione S-transferase omega-1	10.54	10.71	20.33	P78417	6	29	2.53	0.56		present	
Myosin light polypeptide 6	17.82	17.91	62.25	P60660	10	38	2.52	0.52		present	
Bifunctional purine biosynthesis protein PURH	21.8	22.16	25.17	P31939	11	12	2.50	0.38		present	
Peroxiredoxin-1	21.75	21.82	49.25	Q06830	12	65	2.36	0.24	NC		
Coactosin-like protein	12.16	12.34	42.96	Q14019	7	21	2.35	0.41	NC		
Transketolase	32.71	34.5	30.50	P29401	20	50	2.23	0.04		present	
Phosphoglycerate mutase 1	14.1	14.17	31.10	P18669	8	28	2.11	0.41		present	
Alpha-actinin-4	110.54	110.54	61.25	O43707	53	187	2.09	0.49		present	
Superoxide dismutase [Cu-Zn]	6.32	6.32	25.32	P00441	4	12	2.02	0.33	NC		
Elongation factor 1-beta	11.48	13.47	24.89	P24534	5	27	2.02	0.63	NC		
14-3-3 protein zeta/delta	31.93	32.22	60.82	P63104	16	67	1.95	0.14		present	
Adenylyl cyclase-associated protein 1	17.87	17.96	20.42	Q01518	8	34	1.91	0.36		present	
L-lactate dehydrogenase A chain	30.52	30.76	45.78	P00338	15	112	1.84	0.13	NC		
Alpha-actinin-1	15.89	52.15	33.41	P12814	12	6	1.83	1.17		present	
Galectin-3-binding protein	23.78	24.24	22.39	Q08380	12	28	1.82	0.24	SP		
Cofilin-1	26.23	26.58	79.52	P23528	14	128	1.76	0.22	NC		
Importin subunit beta-1	34.77	36.42	27.97	Q14974	18	26	1.72	0.38	NC		
Triosephosphate isomerase	32.93	32.93	63.29	P60174	18	97	1.60	0.05	NC		
Non-histone chromosomal protein HMG-17	5.02	5.02	22.22	P05204	3	9	1.57	0.40	NC		
Heat shock 70 kDa protein 4	39.86	41.48	33.93	P34932	20	12	1.55	0.61		present	

[a] Average of four iTRAQ CM CSC / CM Panc1 ratios, i.e. 116/114, 121/118, 116/118, and 121/114. The ratios were followed by the corresponding standard deviation (sd). [b] SecretomeP prediction for non-classical secretion (NC). Classically secreted proteins would contain the N-terminal signal peptide (SP) while proteins predicted to be neither classically nor non-classically secreted were further analyzed by Exocarta and Vesiclepedia. [c] Prediction of exosomal release via manual annotation against the Exocarta database. Proteins that were not classically secreted and were present in the database were labeled "present". [d] Prediction of extracellular vesicles release via manual annotation against the Vesiclepedia database. Proteins that were not classically secreted and were present in the database were labeled "present".

Table 2. Secreted proteins with higher abundance in the CM of Panc1 cells compared to Panc1 CSCs.

Name	Unused	Total	% Seq Coverage (95)	UniProt/Swiss Prot Accession	Peptides (> 93.8%)	Peptides used for quant	Average CM CSCs/ Panc1 (< 0.667) [a]	sd	SecretomeP [b]	ExoCarta [c]
Alpha-2-HS-glycoprotein	6	7.28	6.81	P02765	3	27	0.02	0.01	SP	
Lactadherin	12.36	12.67	24.81	Q08431	7	8	0.03	0.01	SP	
Serum albumin	39.03	39.77	28.41	P02768	19	104	0.03	0.00	SP	
Alpha-2-macroglobulin	6.83	8.35	2.17	P01023	3	5	0.03	0.02	SP	
Plasminogen activator inhibitor 1	33.24	33.47	45.02	P05121	18	67	0.08	0.03	SP	
Brain acid soluble protein 1	26.36	26.36	78.41	P80723	13	113	0.09	0.02		present
Neural cell adhesion molecule L1	8.61	10.24	7.56	P32004	7	2	0.10	0.04	SP	
Transforming growth factor-beta-induced protein ig-h3	15.94	18.78	15.52	Q15582	9	28	0.11	0.02	SP	
Collagen alpha-1(XVIII) chain	25.83	26.68	10.43	P39060	14	24	0.12	0.06	SP	
Urokinase-type plasminogen activator	9.01	9.4	12.99	P00749	5	5	0.14	0.06	SP	
ADM	2.04	2.04	5.95	P35318	1	2	0.19	0.02	SP	
Protein FAM3C	7.47	7.51	22.47	Q92520	4	5	0.19	0.05	NC	
Transgelin-2	19.51	19.51	57.29	P37802	10	9	0.28	0.20	NC	
Dystroglycan	11.73	12.06	8.94	Q14118	6	14	0.32	0.04	SP	
Laminin subunit beta-1	14.52	21.37	5.04	P07942	7	4	0.37	0.06	SP	
Metalloproteinase inhibitor 2	4.91	4.96	16.82	P16035	4	5	0.39	0.12	SP	
Calsyntenin-1	11.61	11.96	8.16	O94985	8	17	0.39	0.11	SP	
Lysyl oxidase homolog 2	2.58	2.68	2.20	Q9Y4K0	2	2	0.39	0.24	SP	
Clusterin	20.35	20.76	25.84	P10909	11	55	0.40	0.03	SP	
Hsp90 co-chaperone Cdc37	7.74	7.98	15.34	Q16543	4	4	0.41	0.25		present
Serotransferrin	27.82	28.14	21.78	P02787	15	23	0.46	0.11	SP	
Heat shock protein HSP 90-alpha	22.36	54.62	33.74	P07900	11	39	0.54	0.29		present
Apolipoprotein E	21.96	22.06	41.32	P02649	11	5	0.54	0.07	SP	
Plasminogen activator inhibitor 1 RNA-binding protein	12.05	12.13	18.38	Q8NC51	6	18	0.57	0.36		present
Annexin A5	38.6	38.6	55.62	P08758	19	120	0.57	0.10	NC	
Keratin, type II cytoskeletal 2 epidermal	11.71	16.09	12.99	P35908	6	4	0.58	0.14		present
Gelsolin	23.88	24.04	20.84	P06396	11	5	0.59	0.02	SP	
Keratin, type II cytoskeletal 1	7.69	17.9	12.11	P04264	5	10	0.63	0.05		present
Nucleobindin-1	22.21	24	29.93	Q02818	12	32	0.65	0.18	SP	

[a] Average of four iTRAQ CM CSC / CM Panc1 ratios, i.e. 116/114, 121/118, 116/118, and 121/114. The ratios were followed by the corresponding standard deviation (sd). [b] SecretomeP prediction for nonclassical secretion (NC). Classically secreted proteins would contain the N-terminal signal peptide (SP) while proteins predicted to be neither classically nor nonclassically secreted were further analyzed by Exocarta and Vesiclepedia. [c] Prediction of exosomal release via manual annotation against the Exocarta database. Proteins that were not classically secreted and were present in the database were labeled "present".

Table 3. IPA-predicted top biological functions for Panc1 and Panc1 CSC secretomes.

Top biological functions (Panc1 secretome)	p values [a] (ranging from)	No. of molecules [b]
Disease and disorders		
Dermatological Diseases and Conditions	5.08E-16 - 6.06E-03	36
Cancer	5.74E-11 - 9.51E-03	80
Gastrointestinal Disease	5.74E-11 - 8.90E-03	50
Hepatic System Disease	5.74E-11 - 6.64E-03	16
Organismal Injury and Abnormalities	3.53E-10 - 9.20E-03	57
Molecular and cellular functions		
Cell Death and Survival	1.51E-16 - 8.46E-03	49
Cellular Growth and Proliferation	1.07E-14 - 9.51E-03	52
Cellular Movement	4.16E-11 - 9.16E-03	35
Cellular Development	1.07E-09 - 9.51E-03	38
Cell Morphology	6.05E-07 - 6.43E-03	31
Physiological System Developement and Fucntion		
Organismal Survival	7.84E-09 - 7.84E-09	13
Cardiovascular System Development and Function	6.05E-07 - 9.51E-03	14
Organismal Development	6.05E-07 - 8.13E-03	21
Tissue Development	6.05E-07 - 8.13E-03	28
Hematological System Development and Function	5.51E-05 - 9.16E-03	14

Top biological functions (Panc1 CSC secretome)	p values (ranging from)	No. of molecules
Disease and disorders		
Dermatological Diseases and Conditions	6.60E-13 - 8.55E-03	27
Metabolic Disease	1.69E-10 - 1.28E-02	26
Neurological Disease	1.32E-09 - 1.28E-02	34
Psychological Disorders	1.32E-09 - 8.55E-03	33
Cancer	1.41E-09 - 1.28E-02	54
Molecular and cellular functions		
Cell Death and Survival	6.63E-12 - 1.28E-02	35
Cellular Movement	4.73E-09 - 1.28E-02	25
Cellular Growth and Proliferation	1.05E-07 - 1.06E-02	32
Cell Morphology	1.49E-07 - 1.28E-02	28
Cellular Development	1.49E-07 - 9.81E-03	23
Physiological System Developement and Fucntion		
Cardiovascular System Development and Function	1.49E-07 - 1.03E-02	12
Organismal Development	1.49E-07 - 1.04E-02	19
Tissue Development	1.49E-07 - 1.28E-02	23
Organismal Survival	1.98E-06 - 3.64E-03	11
Hematological System Development and Function	4.14E-05 - 1.12E-02	10

[a] Fisher's exact test was used to calculate a p value for each protein of the dataset identified in the biological function studied, indicating the probability that each biological function assigned to the data set is assigned by chance; then we have a range of p values corresponding to all p values calculated for all proteins of the dataset in the biological function. [b] The number of molecules of the differentially released protein dataset is shown.

Figure 1

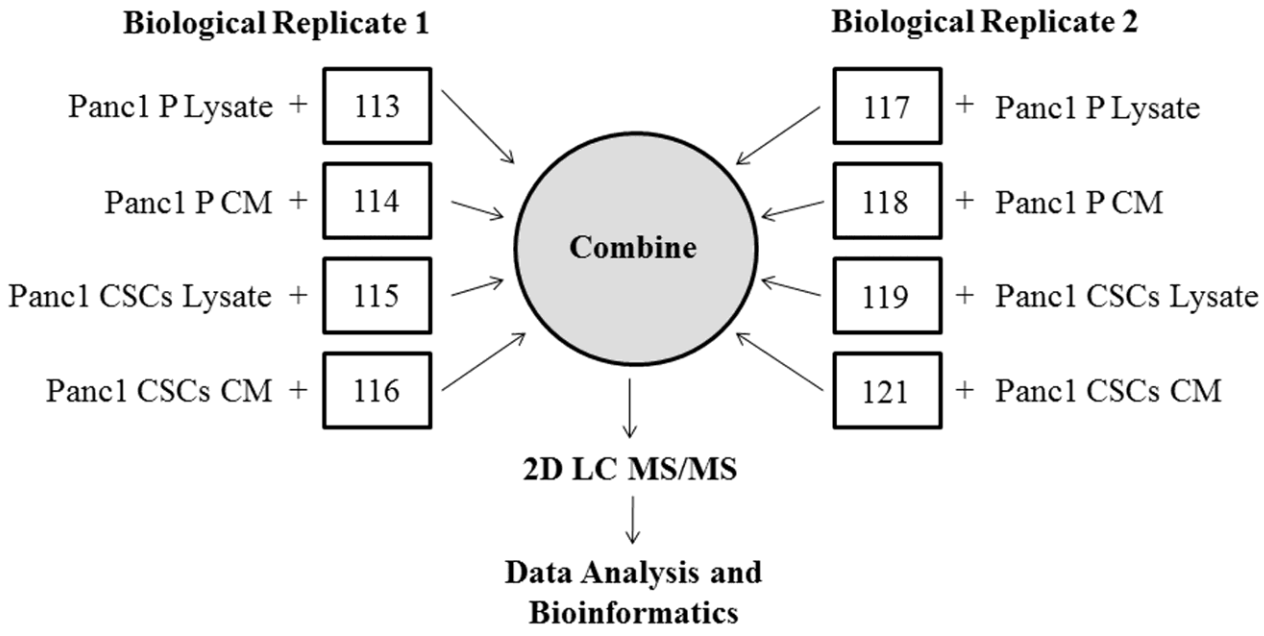

Figure 2

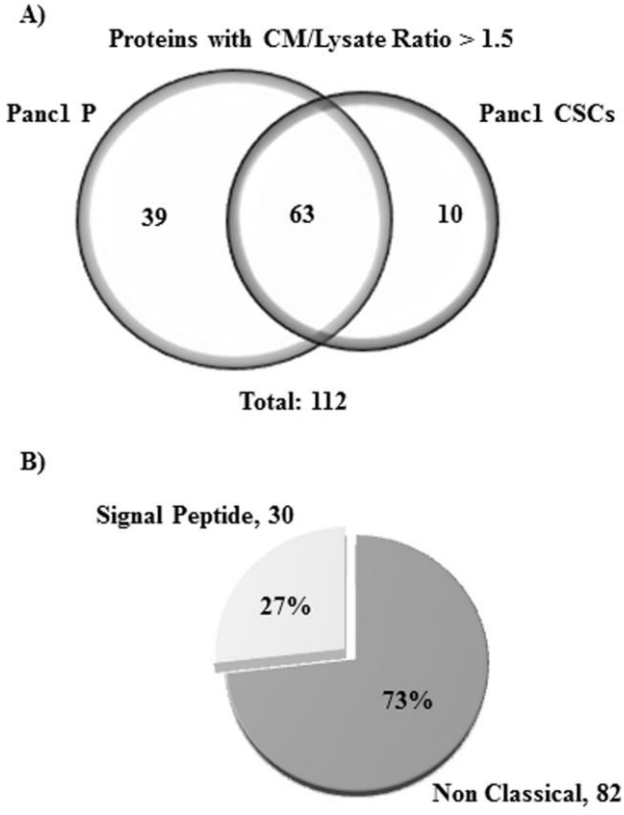

Figure 3

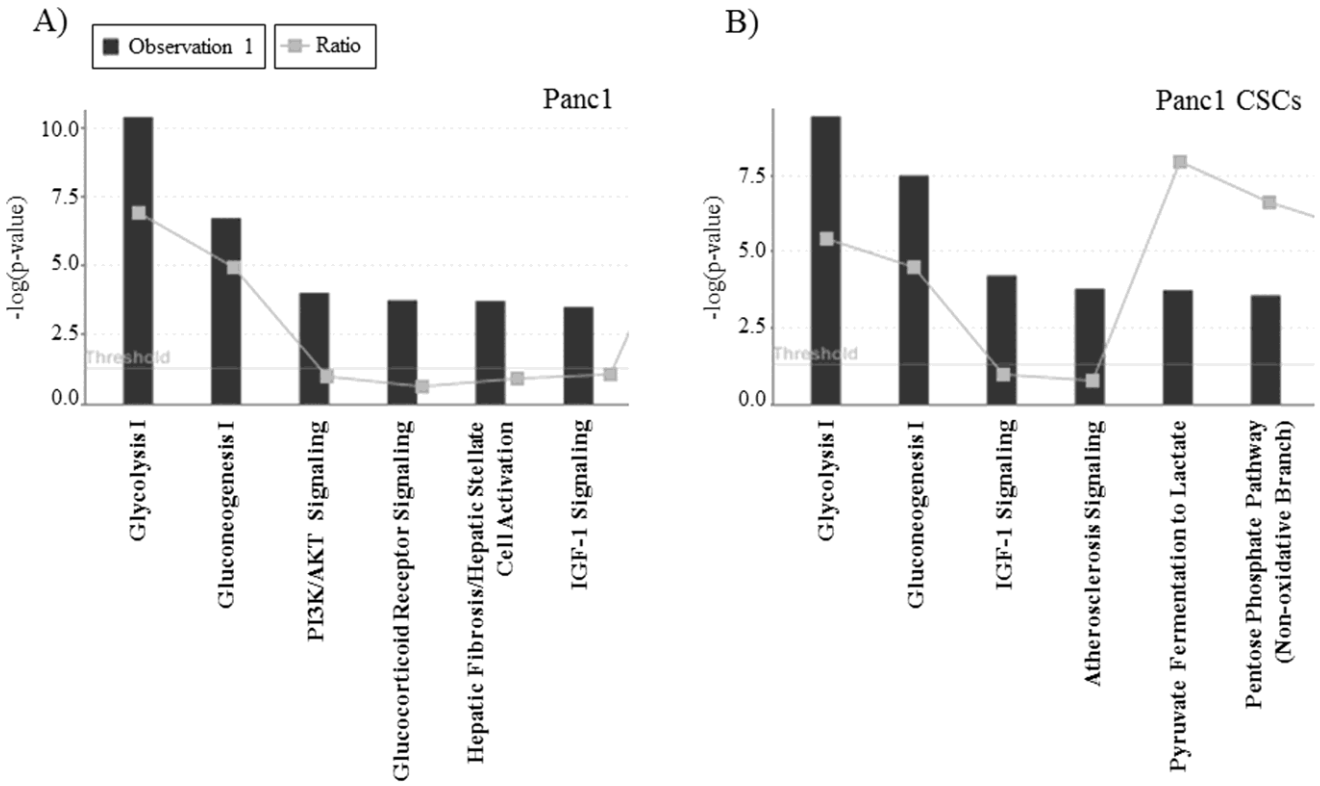
A)
Observation 1
Ratio
Panc1
-log(p-value)
10.0
7.5
5.0
2.5
0.0
Threshold
Glycolysis I
Gluconeogenesis I
PI3K/AKT Signaling
Glucocorticoid Receptor Signaling
Hepatic Fibrosis/Hepatic Stellate Cell Activation
IGF-1 Signaling
B)
Panc1 CSCs
-log(p-value)
7.5
5.0
2.5
0.0
Threshold
Glycolysis I
Gluconeogenesis I
IGF-1 Signaling
Atherosclerosis Signaling
Pyruvate Fermentation to Lactate
Pentose Phosphate Pathway (Non-oxidative Branch)

Figure 4

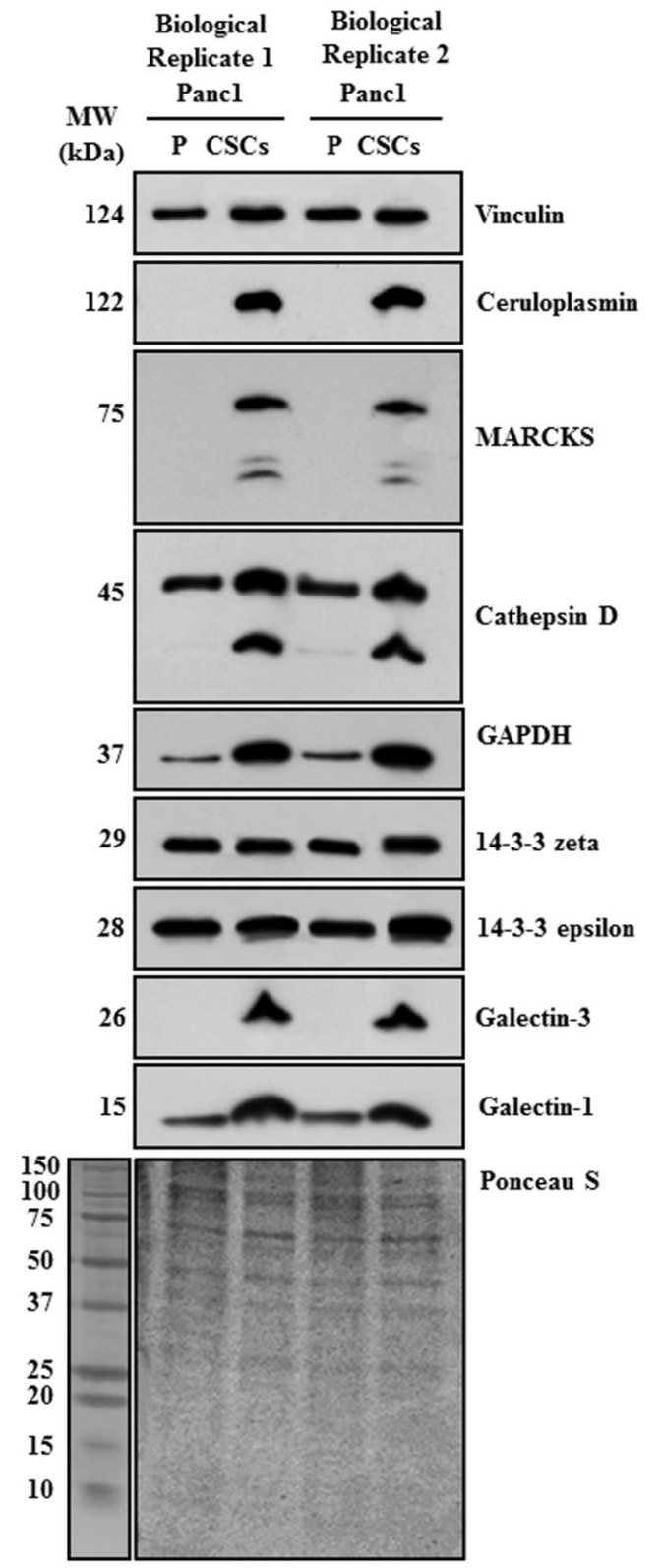
Biological Replicate 1 Panc1
Biological Replicate 2 Panc1
MW (kDa)
P CSCs
P CSCs
124
Vinculin
122
Ceruloplasmin
75
MARCKS
45
Cathepsin D
37
GAPDH
29
14-3-3 zeta
28
14-3-3 epsilon
26
Galectin-3
15
Galectin-1
150
100
75
50
37
25
20
15
10
Ponceau S

Figure 5

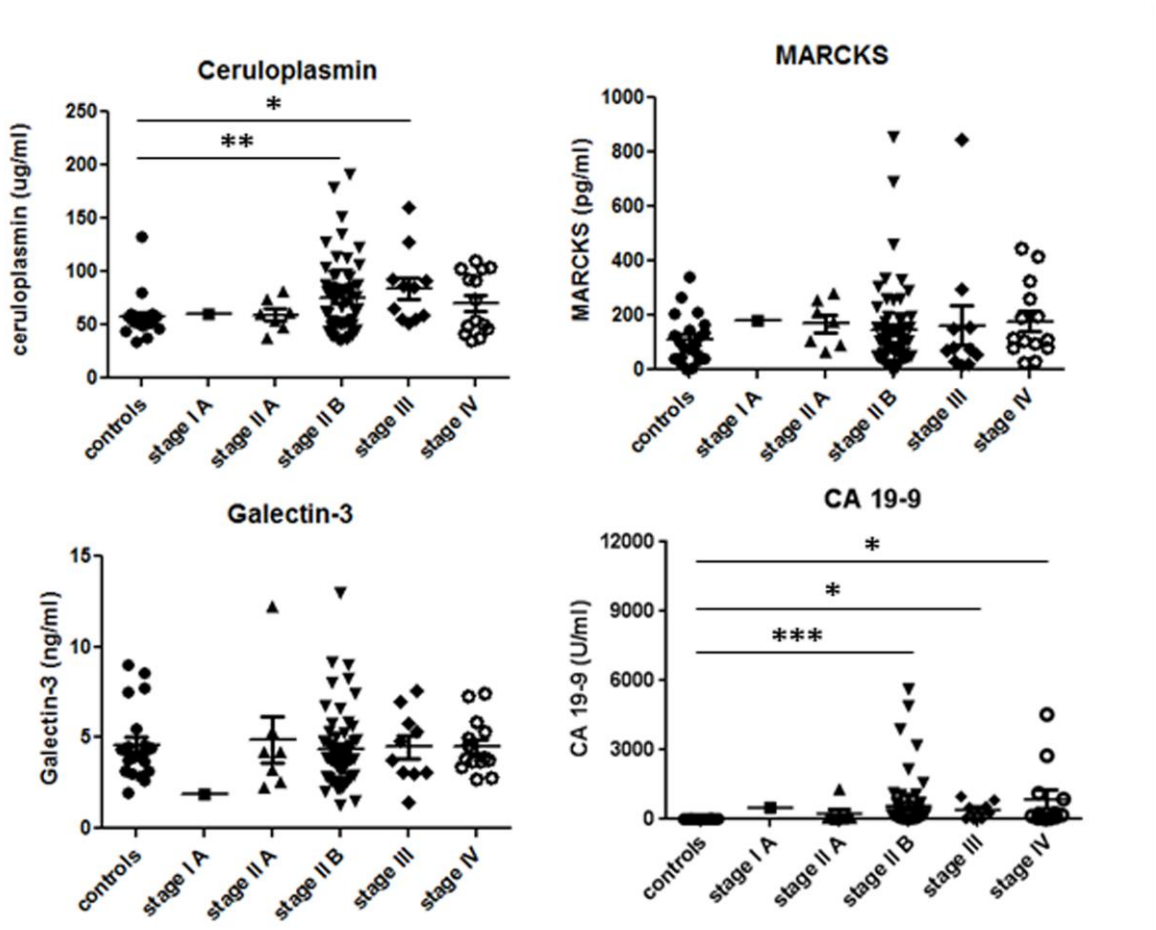
Ceruloplasmin
ceruloplasmin (ug/ml)
250
200
150
100
50
0
*
**
controls
stage I A
stage II A
stage II B
stage III
stage IV
MARCKS
MARCKS (pg/ml)
1000
800
600
400
200
0
controls
stage I A
stage II A
stage II B
stage III
stage IV
Galectin-3
Galectin-3 (ng/ml)
15
10
5
0
controls
stage I A
stage II A
stage II B
stage III
stage IV
CA 19-9
CA 19-9 (U/ml)
12000
9000
6000
3000
0
*
*
***
controls
stage I A
stage II A
stage II B
stage III
stage IV

844 **Figure 6**

845

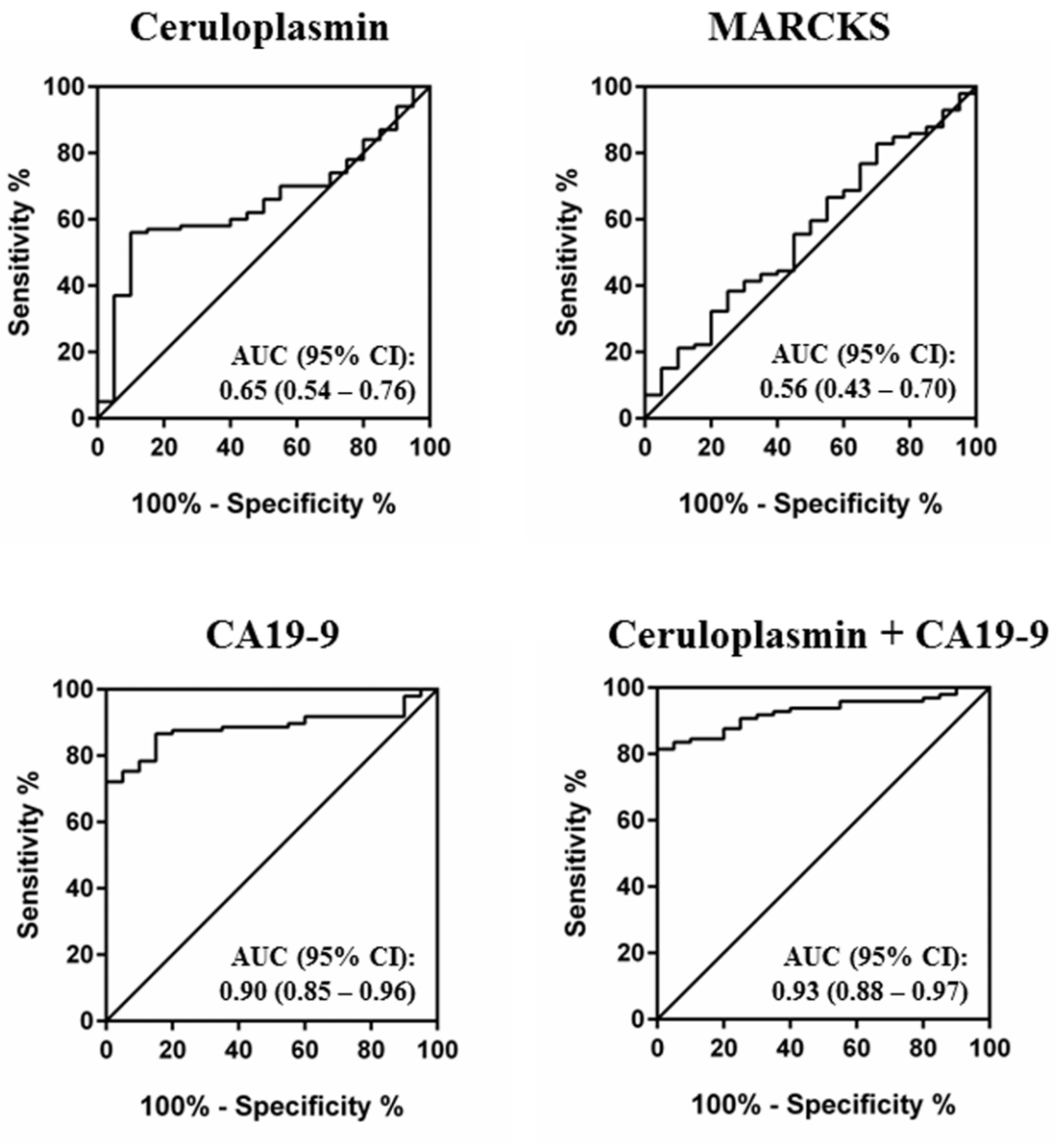

846

847

Figure 1

Click here to download high resolution image

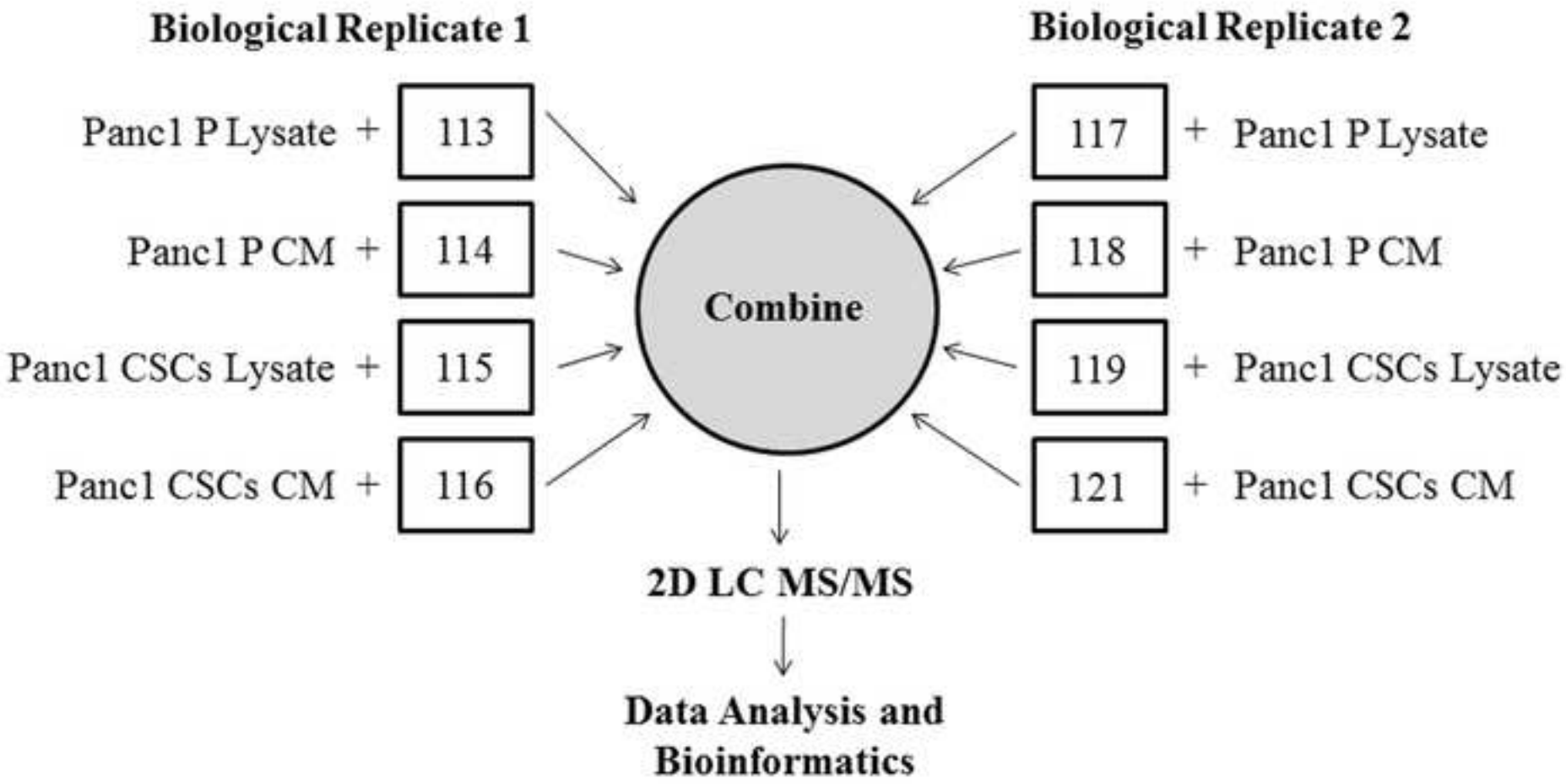

Figure 2
Click here to download high resolution image

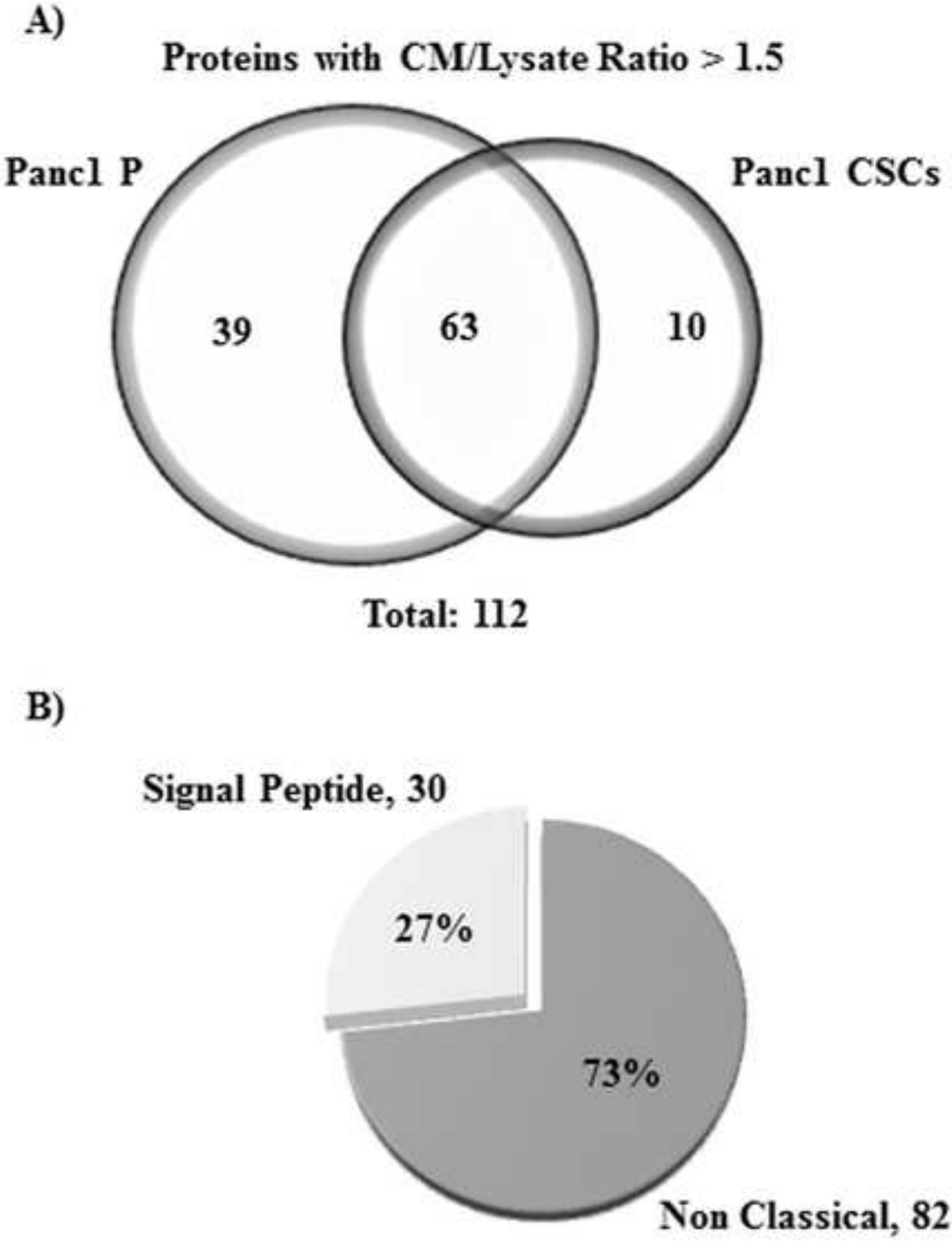

Figure 3

Click here to download high resolution image

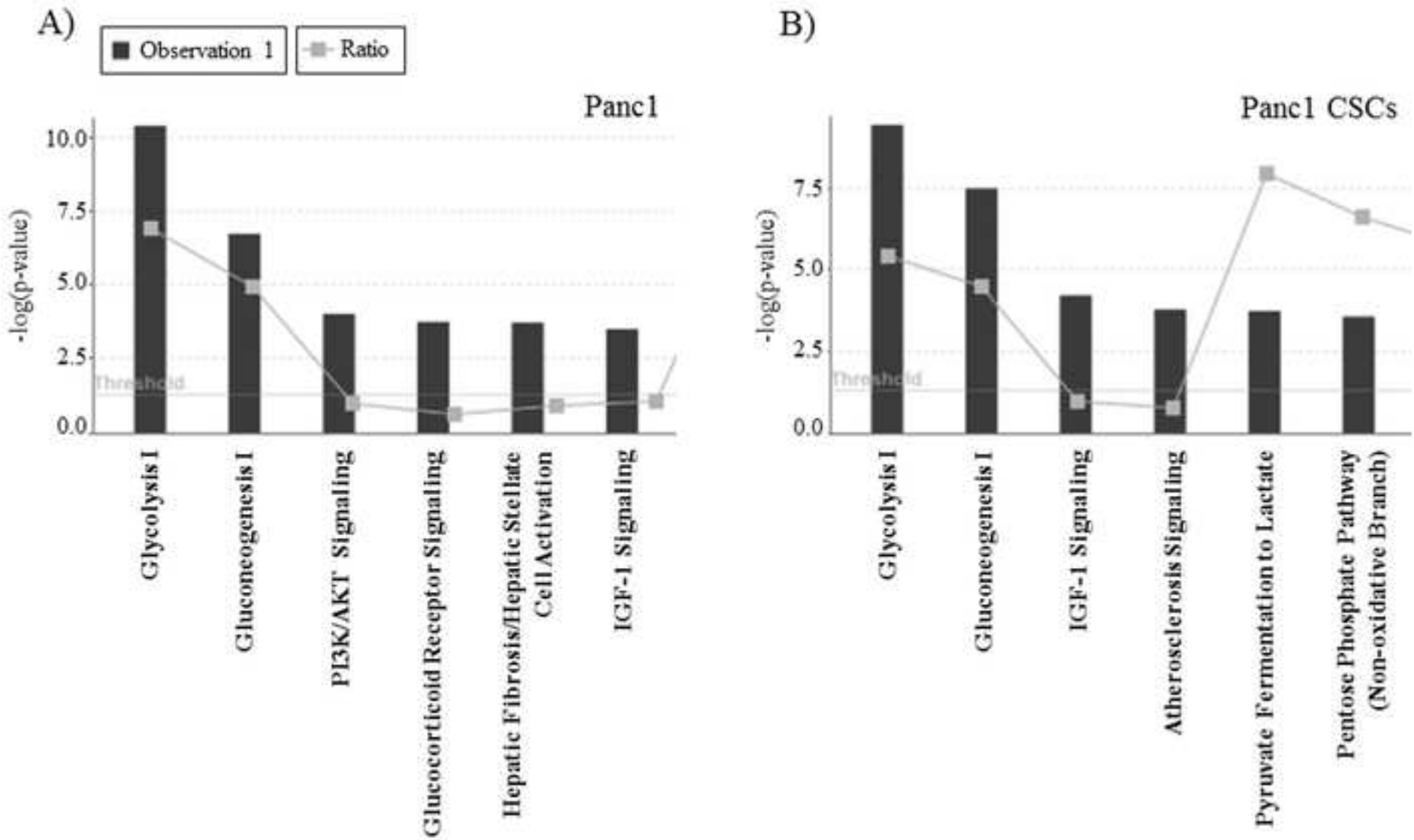

Figure 4

Click here to download high resolution image

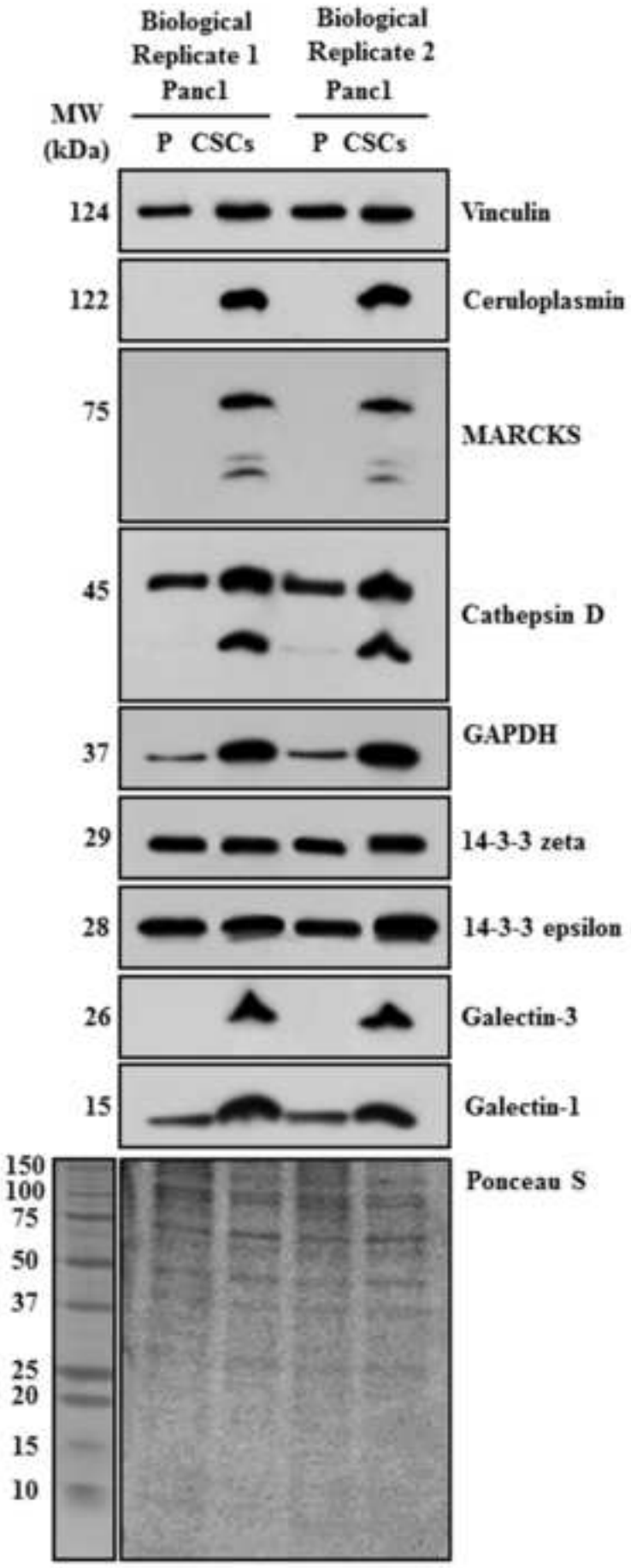

Figure 5 revised2

Click here to download high resolution image

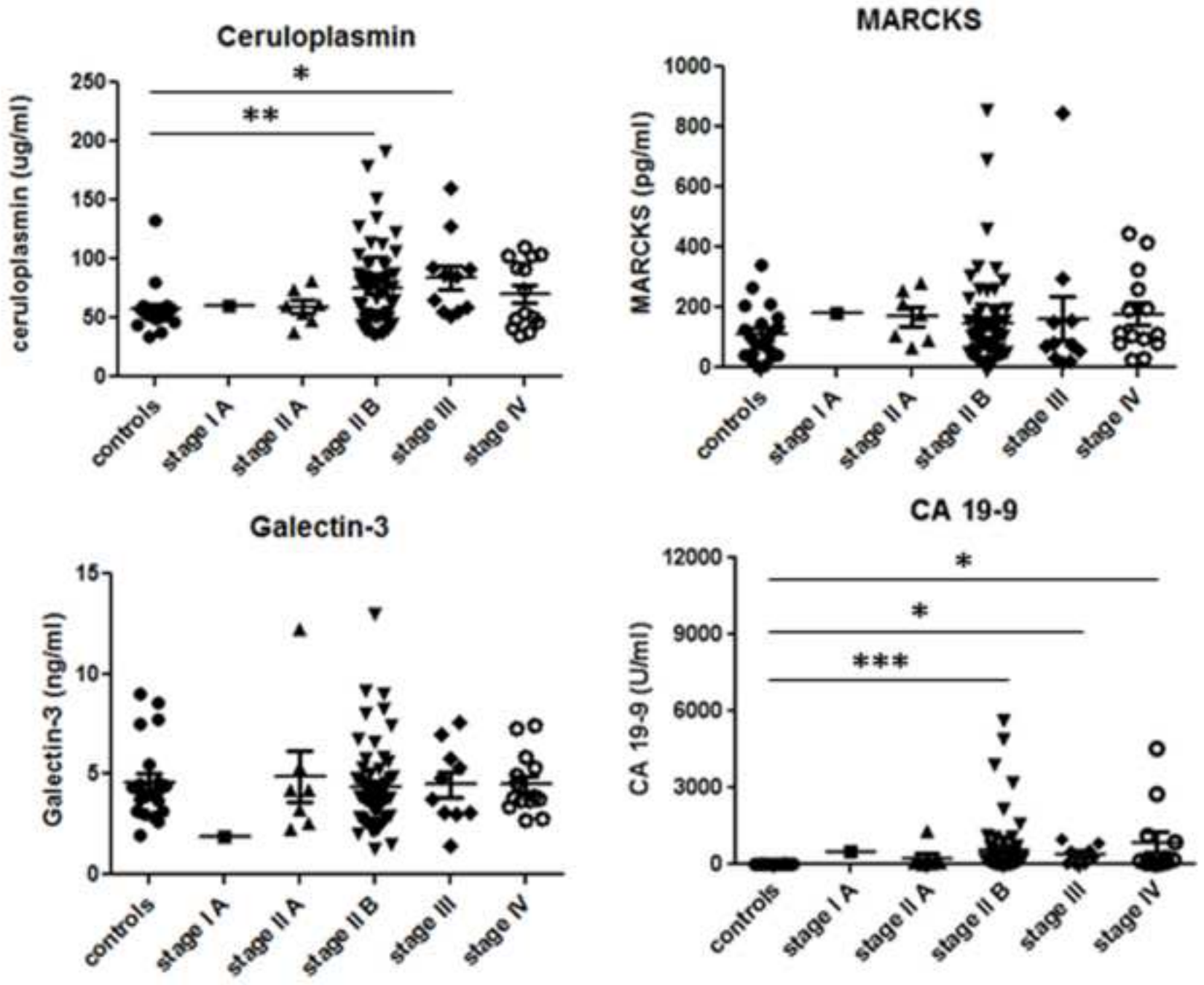

Figure 6
Click here to download high resolution image

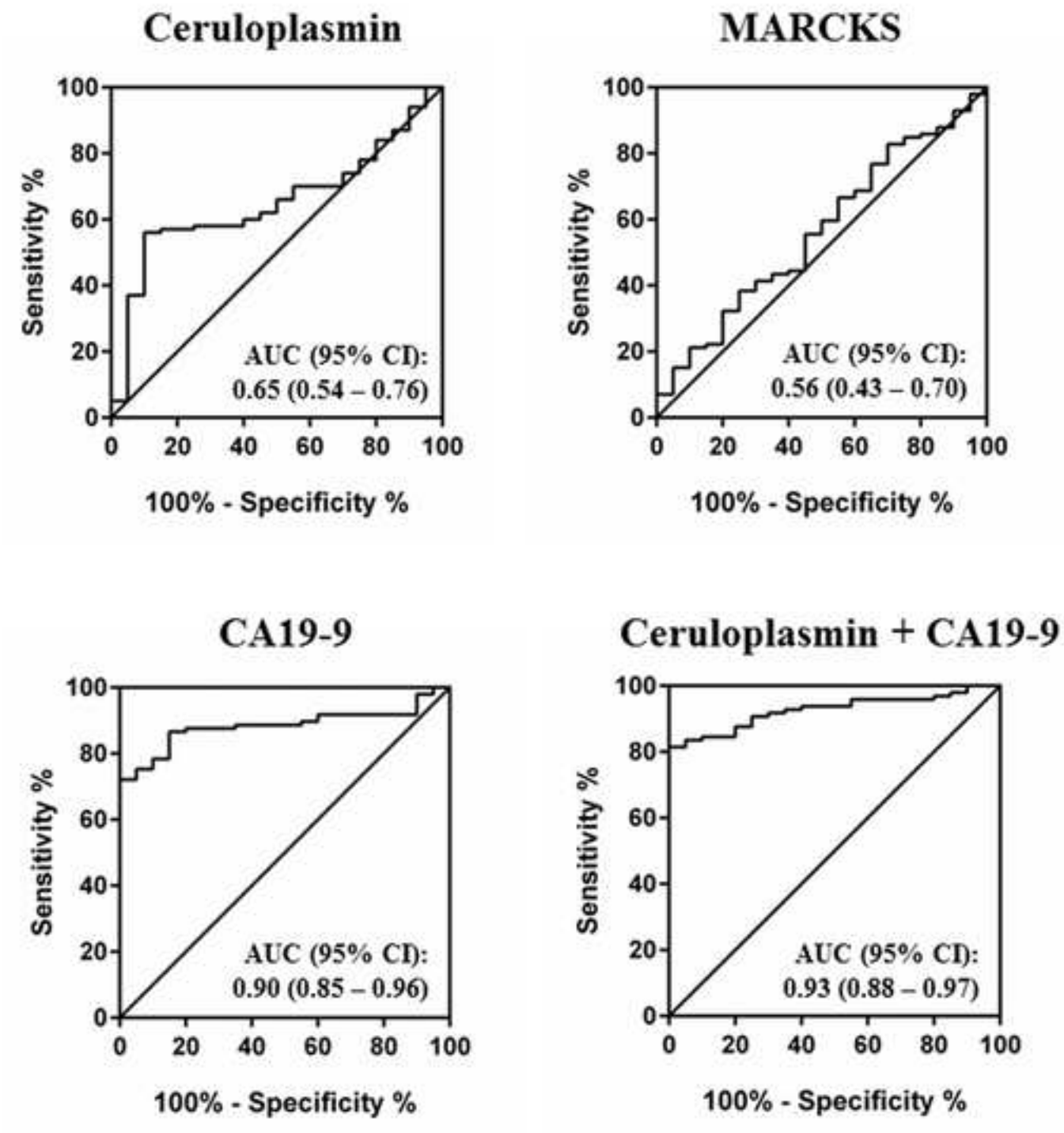

Suppl fig.1

Click here to download Supplementary material: supplemental Figure 1 (networks alterations).doc

Suppl. fig.2

Click here to download Supplementary material: supplemental Figure 2 (scheme of ceruloplasmin).doc

Supplementary tab1

Click here to download Supplementary material: supplemental Table 1 (antibodies used for western blotting validation).doc

Supplementary tab2

Click here to download Supplementary material: supplemental Table 2 (clinical features PDAC patients).doc

Supplementary tab3

Click here to download Supplementary material: Supplemental Table 3 (2045 identified proteins, 1157 quantified proteins).xls

Supplementary tab4

Click here to download Supplementary material: Supplemental Table 4 (n=608 identification via single peptide).xls

Supplementary tab5

Click here to download Supplementary material: Supplemental Table 5 (112 secreted proteins).xls

Supplementary tab6

Click here to download Supplementary material: supplemental Table 6 (pathways enriched).doc

Supplementary tab7

Click here to download Supplementary material: supplemental Table 7 (correlations markers with clinicopathology).doc

Brandi et al- J of Proteomics (changes highlightes)

Click here to download Supplementary material: Brandi et al- J of Proteomics (changes highlightes).docx

Suppl material ONLY for reviewer

Click here to download Supplementary material: Suppl material for reviewer.tif

***Conflict of Interest**

Click here to download Conflict of Interest: Conflict of interest.docx